Intramolecular Hydrogen Bond-controlled Prolyl Amide Isomerization in Glucosyl 3(*S*)-hydroxy-5′-hydroxymethyl Proline Hybrids – The Influence of a C-5′-hydroxymethyl Substituent on the Thermodynamics and Kinetics of Prolyl Amide Cis/Trans Isomerization.

Kaidong Zhang[†], Robel B. Teklebrhan[†], George Schreckenbach[†], Stacey Wetmore[‡] and Frank Schweizer[†,*]

[†]*Department of Chemistry, University of Manitoba, Winnipeg, Manitoba R3T 2N2 Canada*

[‡]*Department of Chemistry & Biochemistry, University of Lethbridge, Lethbridge, Alberta T1K 3M4 Canada*

**schweize@cc.umanitoba.ca*

Table of Contents

Experimental Procedure

General

^{1}H and ^{13}C NMR spectra were taken in CD_3OD, D_2O at 500 MHz and 75 MHz NMR spectrometer, respectively. 1D NOE experiments (40ms gaussian pulse with a 560ms mixing time) and HSQC experiments were performed at 500 MHz NMR spectrometer. The data from Inversion-Magnetization Transfer experiment were processed by Mathematica 5.0. Analytical thin layer chromatography was performed on 0.20 mm silica gel 60 Å plates. Flash chromatography was performed on 40-63 μm 60 Å silica gel.

.

Synthetic procedure for compounds 7 and 8

(1*S*)-2,3,4,6-Tetrahydroxy-1′-*N*-acetyl-5′(*S*)-hydroxymethylene-spiro[1,5-anhydro-D-glucitol-1,3′-*L*-proline methylamide] (**7**). Compound **3** (25 mg, 0.07 mmol) was dissolved in a solution of methylamine in absolute ethanol (4 mL, 33% wt) and stirred for 18 hours at room temperature. The mixture was concentrated and purified by the flash column chromatography (dichloromethane/ methanol: 2/1) to get compound **7** as a colorless oil (23 mg, 95%)

(1*S*)-2,3,4,6-Tetrahydroxy-1′-*N*-acetyl-5′(*R*)- hydroxymethylene-spiro[1,5-anhydro-D-glucitol-1,3′-*L*-proline methylamide] (**8**). Compound **4** (30 mg, 0.09 mmol) was dissolved in a solution of methylamine in absolute ethanol (4.5 mL, 33% wt) and stirred for 18 hours at room temperature. The mixture was concentrated and purified by the flash column chromatography (dichloromethane/ methanol: 2/1) to get compound **8** as a colorless oil (28 mg, 93%)

^{1}H and ^{13}C NMR Spectra for compound 3-8 in D_2O

Compound **3**

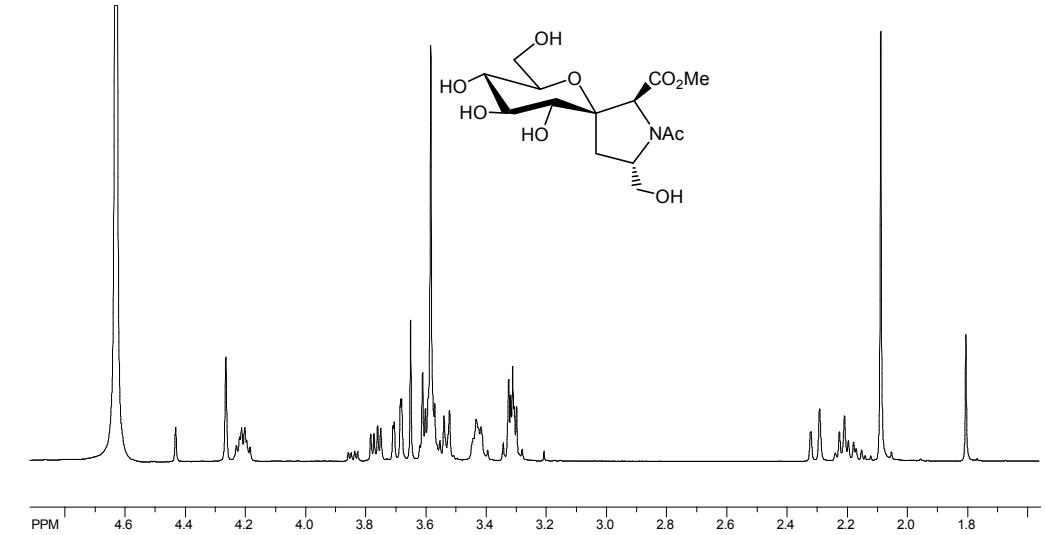

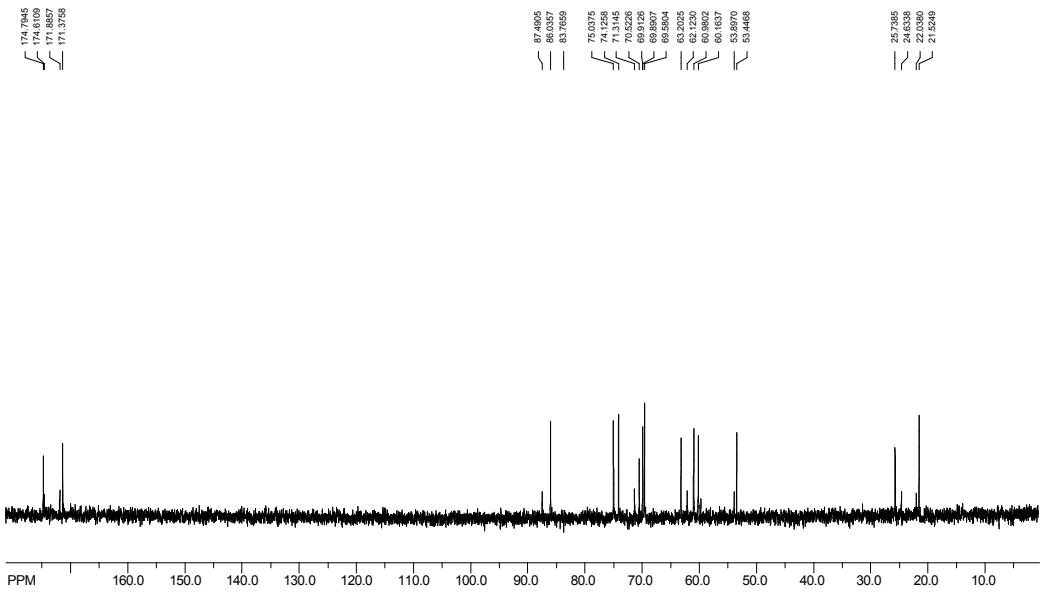

Compound **4**

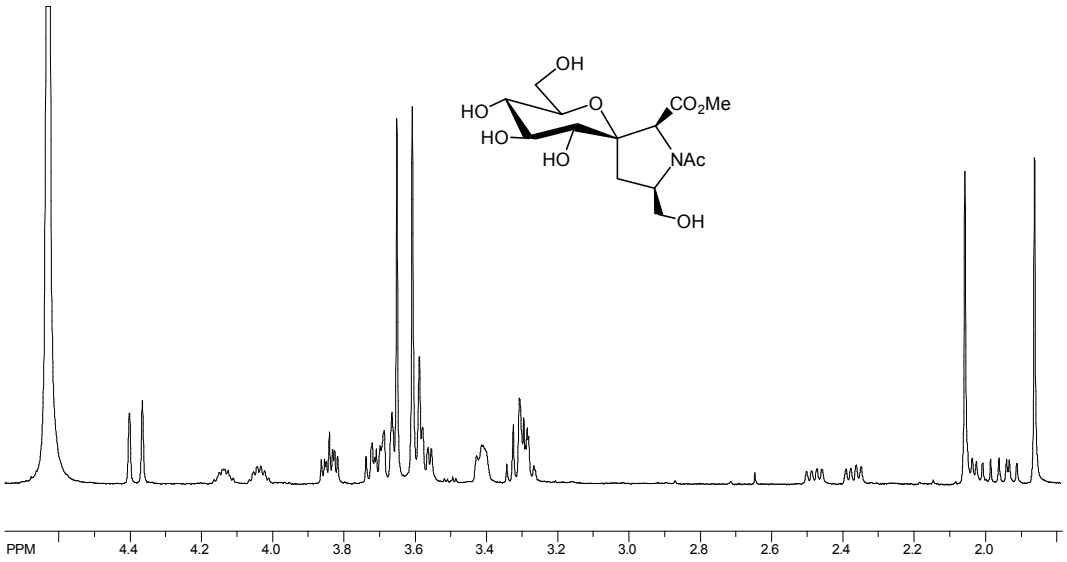
OH
HO
O
CO2Me
HO
HO
NAc
OH
PPM
4.4
4.2
4.0
3.8
3.6
3.4
3.2
3.0
2.8
2.6
2.4
2.2
2.0

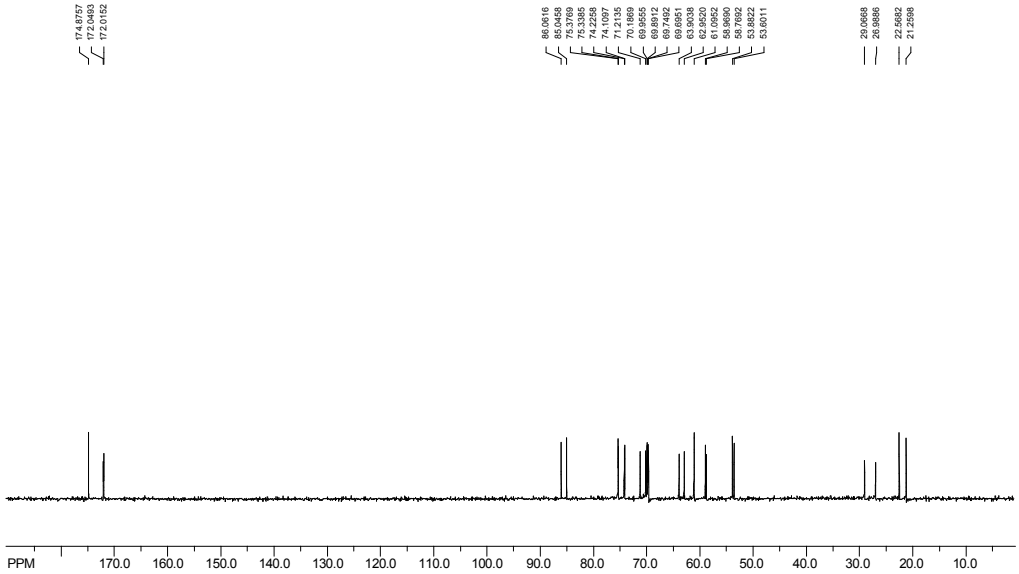
174.8757
172.0493
172.0152
86.0616
85.0458
75.3769
75.3385
74.2258
74.1097
71.1435
70.1869
69.9555
69.8812
69.7492
69.6951
63.9038
62.9520
61.0952
58.9690
58.7692
53.8822
53.6011
29.0668
26.9886
22.5682
21.2598
PPM
170.0
160.0
150.0
140.0
130.0
120.0
110.0
100.0
90.0
80.0
70.0
60.0
50.0
40.0
30.0
20.0
10.0

Compound **5**

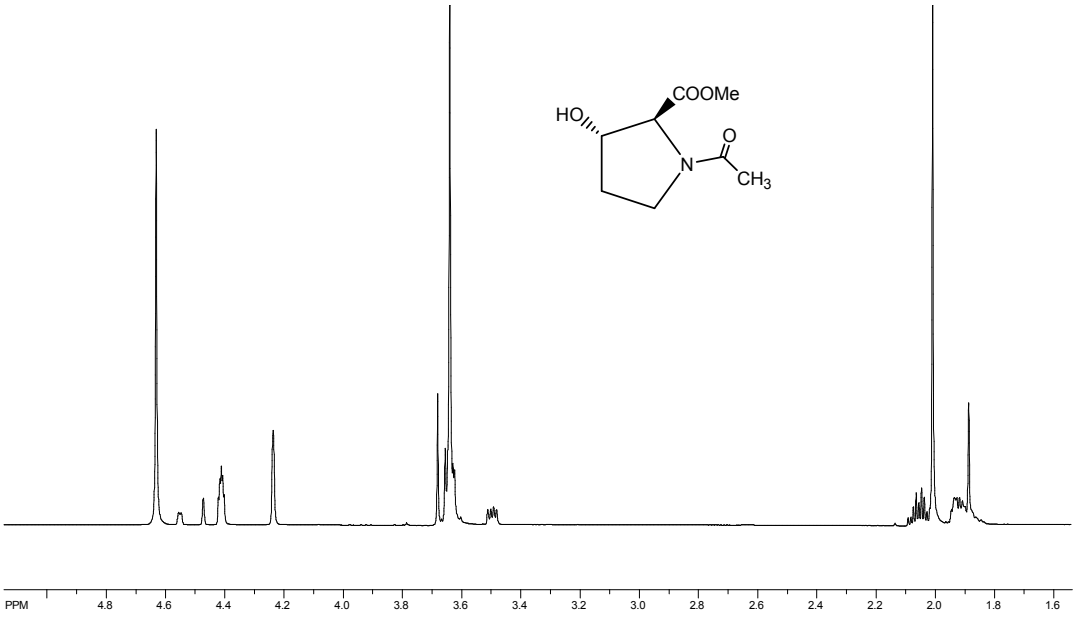
COOMe
HO
O
N
CH3
PPM
4.8
4.6
4.4
4.2
4.0
3.8
3.6
3.4
3.2
3.0
2.8
2.6
2.4
2.2
2.0
1.8
1.6

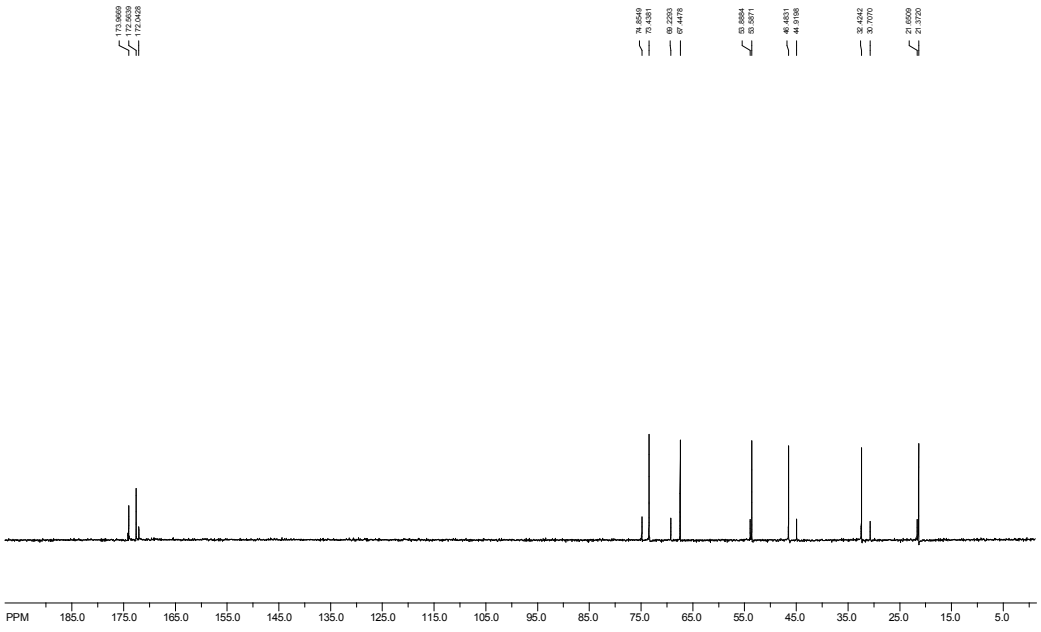
PPM
185.0
175.0
165.0
155.0
145.0
135.0
125.0
115.0
105.0
95.0
85.0
75.0
65.0
55.0
45.0
35.0
25.0
15.0
5.0

Compound **6**

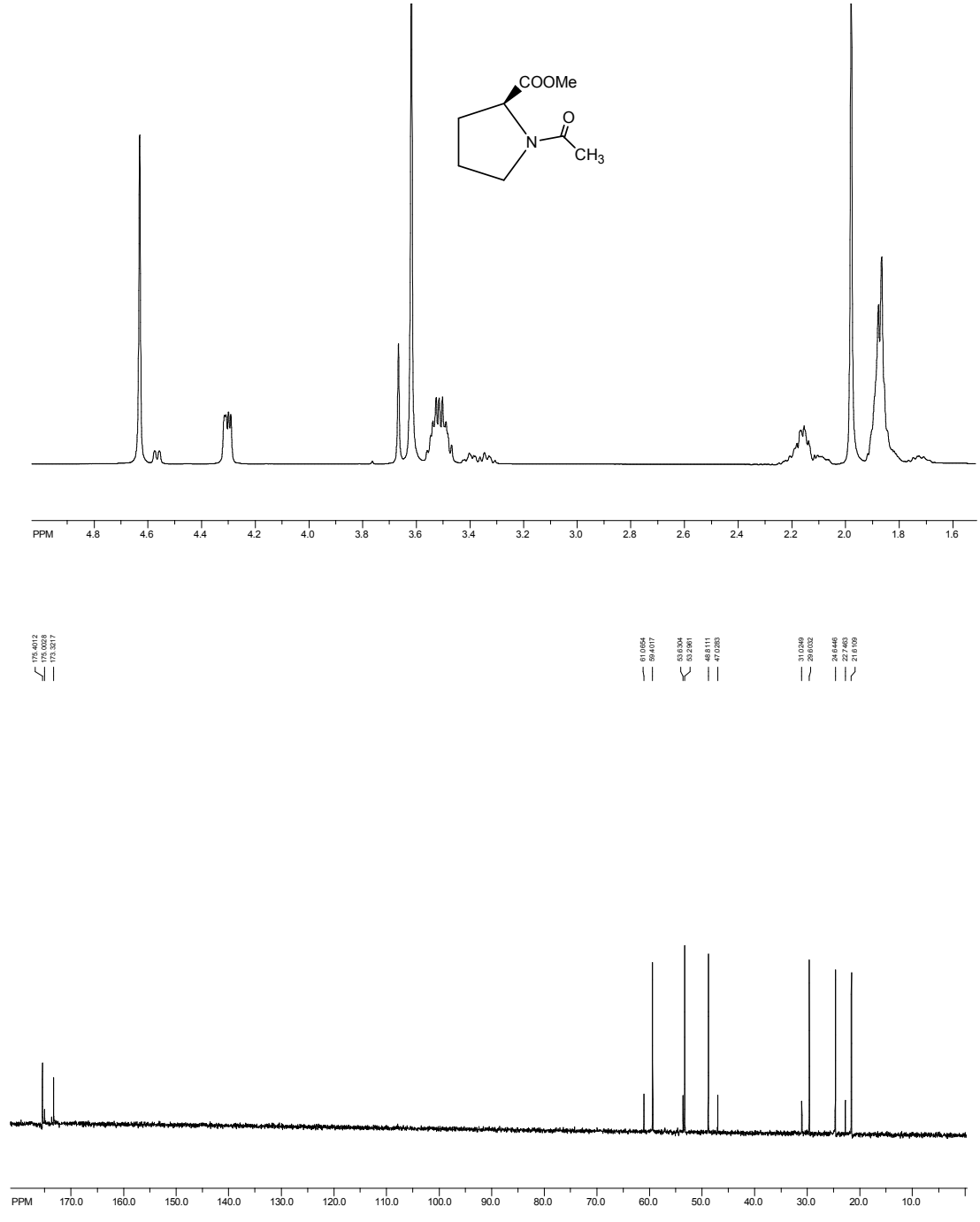
COOMe
O
N
CH3
PPM
4.8
4.6
4.4
4.2
4.0
3.8
3.6
3.4
3.2
3.0
2.8
2.6
2.4
2.2
2.0
1.8
1.6
175.4012
175.0709
173.3217
61.0654
59.4077
53.6304
53.2961
48.8111
47.0283
31.0249
29.8552
24.5446
22.7463
21.6109
PPM
170.0
160.0
150.0
140.0
130.0
120.0
110.0
100.0
90.0
80.0
70.0
60.0
50.0
40.0
30.0
20.0
10.0

Compound **7**

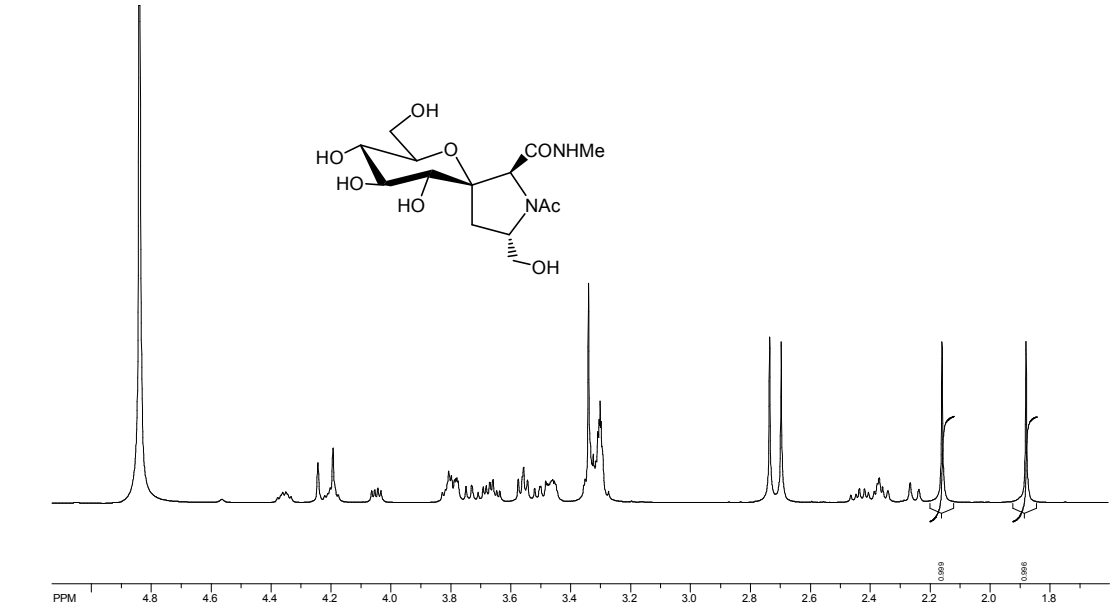
OH
HO
HO
HO
O
CONHMe
NAc
OH
0.999
0.998
PPM
4.8
4.6
4.4
4.2
4.0
3.8
3.6
3.4
3.2
3.0
2.8
2.6
2.4
2.2
2.0
1.8

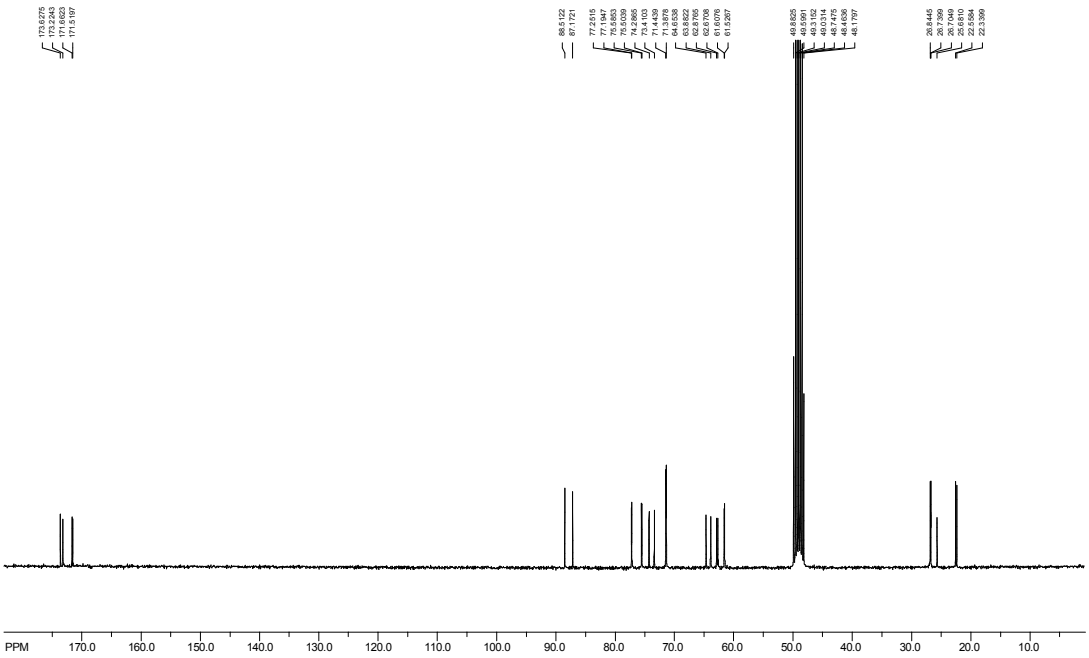
171.6075
173.2243
171.6823
171.5197
86.5122
67.1721
77.2915
77.1447
76.9580
75.5039
74.2865
73.4103
71.4498
71.3878
64.6538
63.2032
62.8765
62.6708
61.6076
61.5267
49.8825
49.5991
49.3132
49.0314
48.7475
48.4636
48.1797
26.8445
26.7399
26.7049
25.6510
22.5584
22.3366
PPM
170.0
160.0
150.0
140.0
130.0
120.0
110.0
100.0
90.0
80.0
70.0
60.0
50.0
40.0
30.0
20.0
10.0

Compound **8**

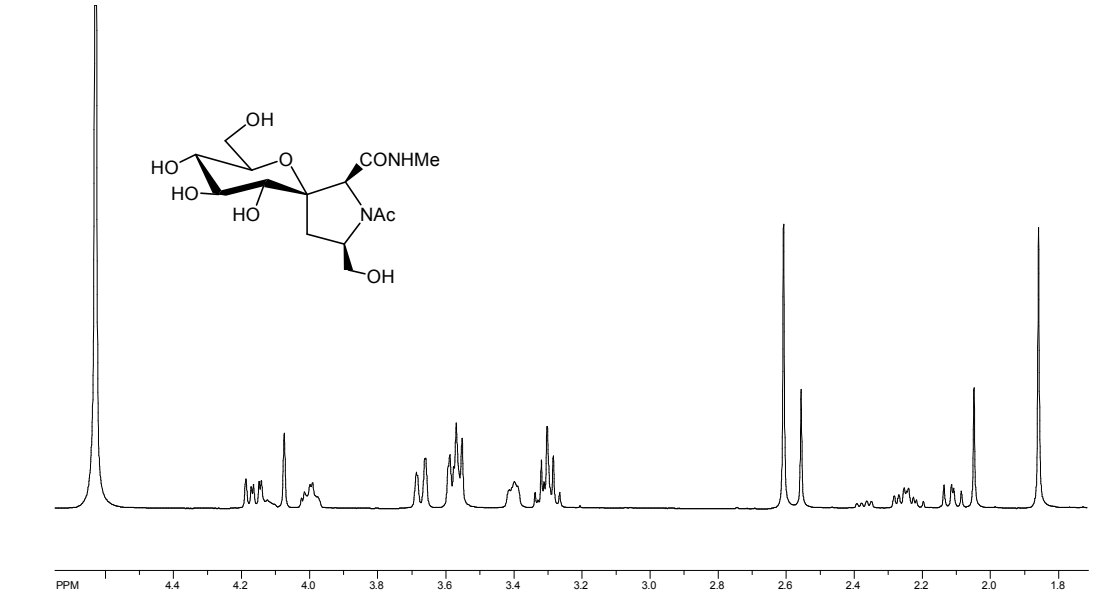
OH
HO
HO
HO
O
CONHMe
NAc
OH
PPM
4.4
4.2
4.0
3.8
3.6
3.4
3.2
3.0
2.8
2.6
2.4
2.2
2.0
1.8

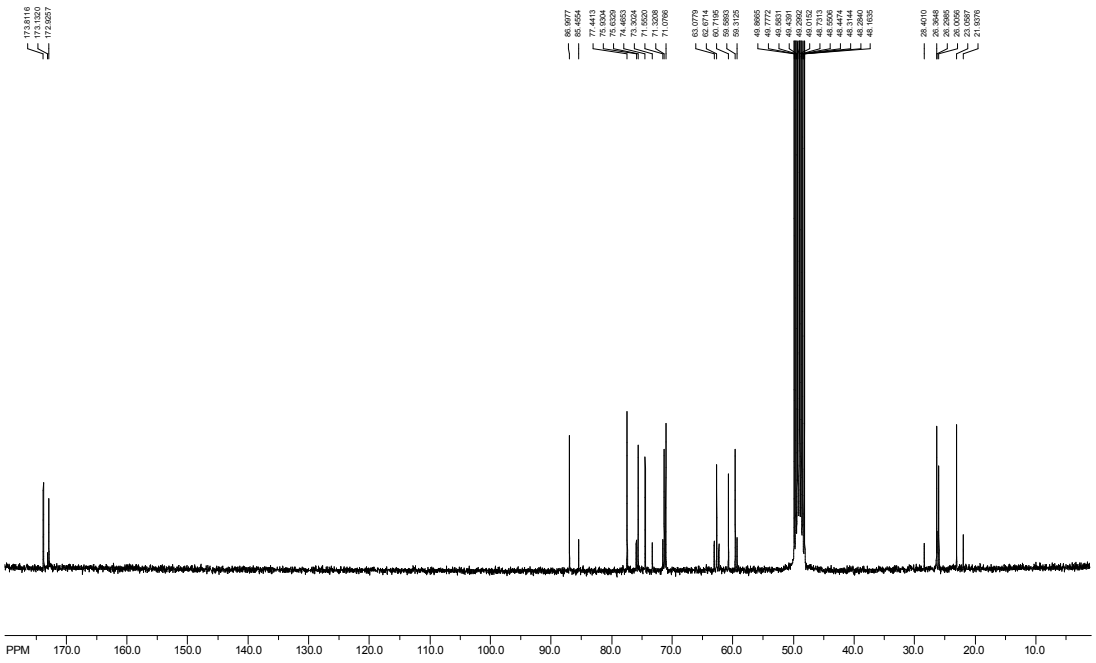
PPM
170.0
160.0
150.0
140.0
130.0
120.0
110.0
100.0
90.0
80.0
70.0
60.0
50.0
40.0
30.0
20.0
10.0

Assignment of *cis* and *trans* rotamers of compounds 3, 4, 7 and 8 through 1D nOe Experiments

Compound **3** in CD_3OD

^1H NMR spectrum

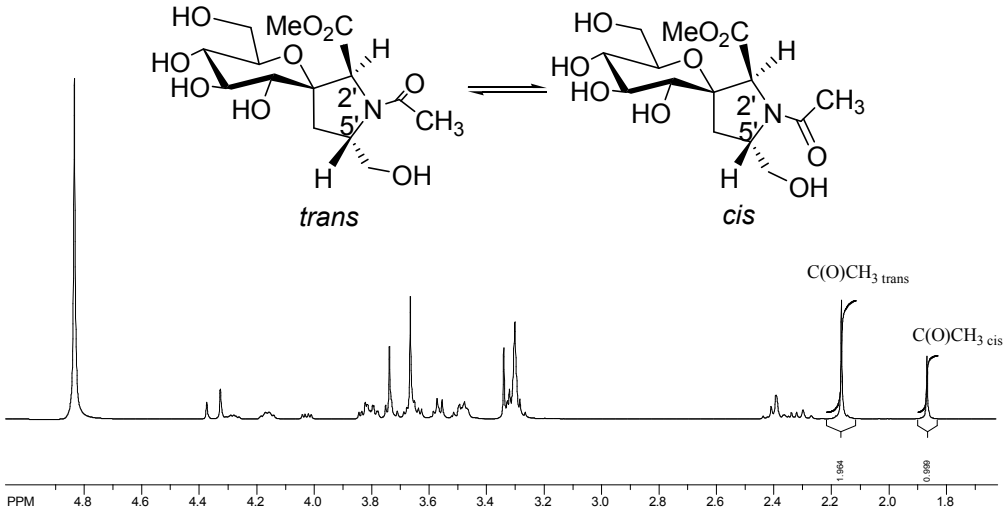

1D nOe spectrum

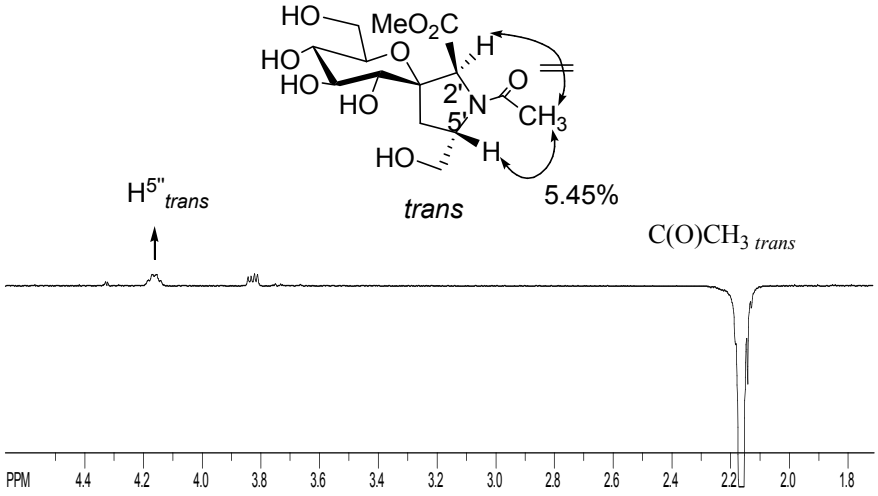

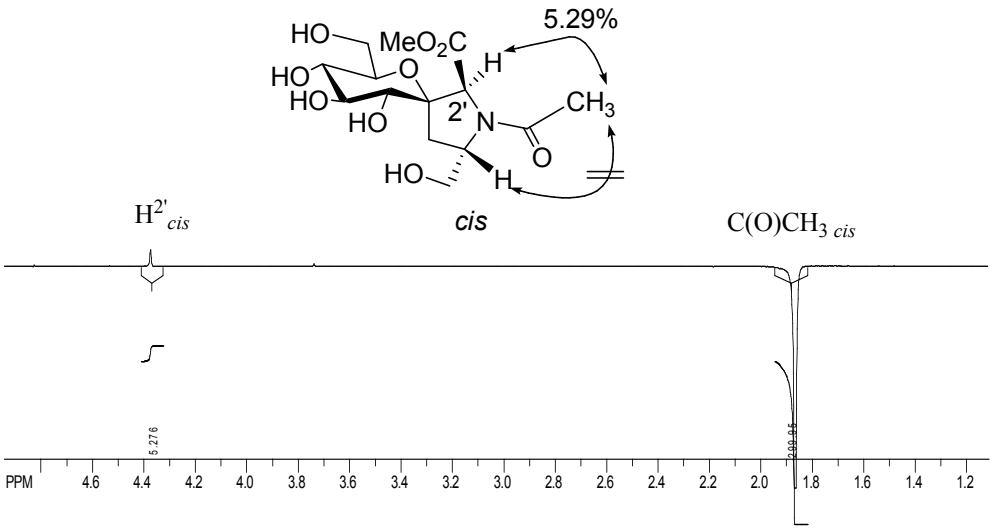

Different Chemical shift of C-2′ (α-carbon) for *cis* and *trans* rotamers of compound 3 in CD_3OD (HSQC)

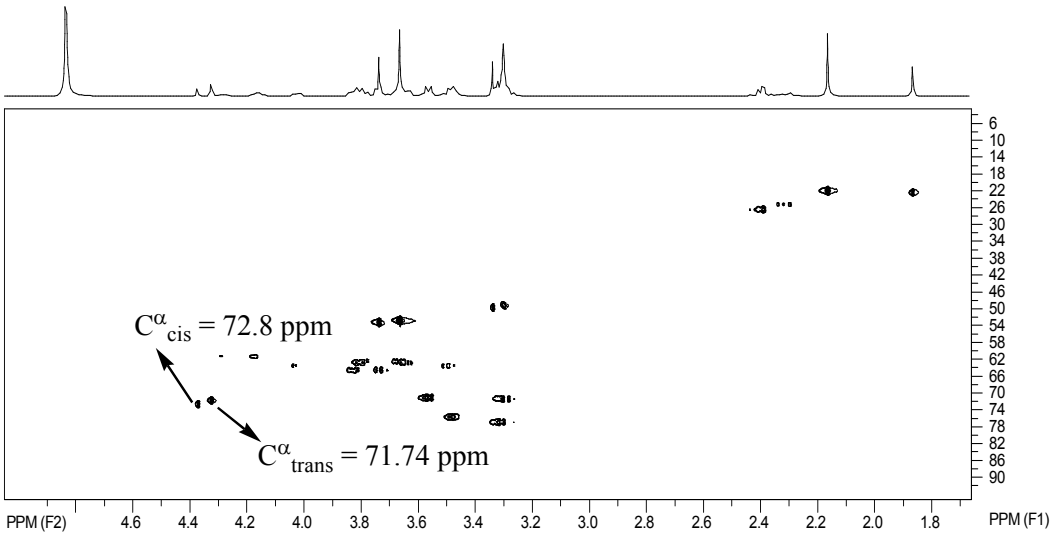

Compound **3** in D_2O

1D nOe spectrum

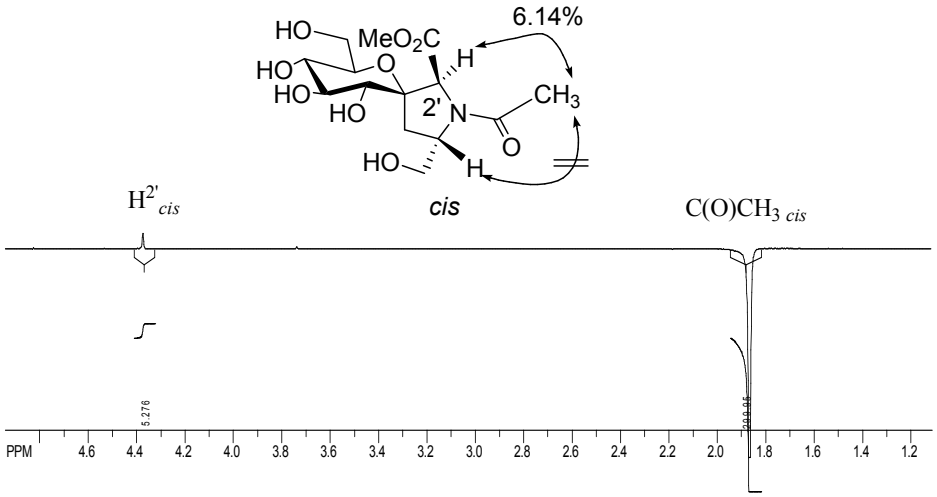

Different chemical shift of C-2′ (α-carbon) for *cis* and *trans* rotamers of compound 3 in D_2O (HSQC)

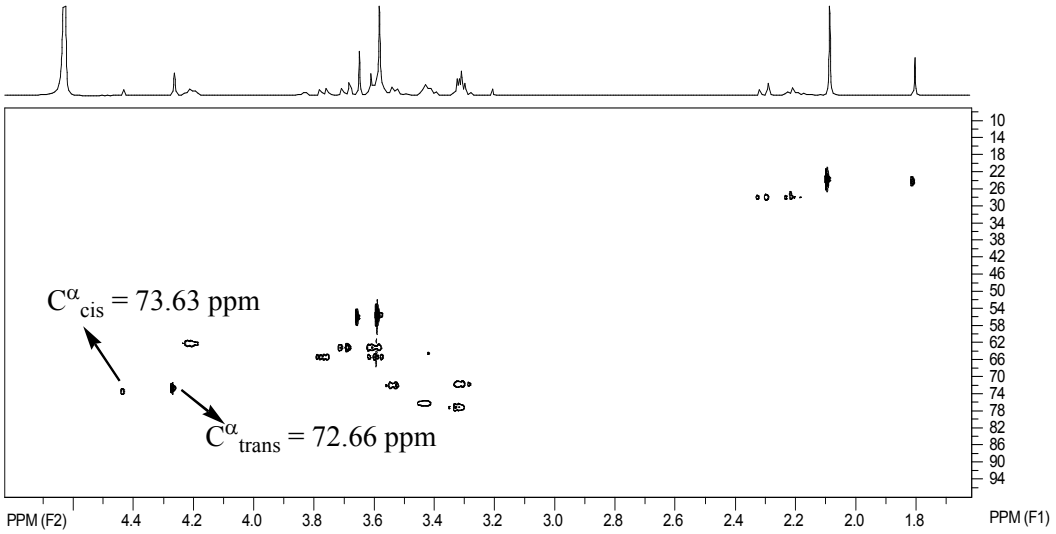

Compound **4** in CD_3OD

^1H NMR spectrum

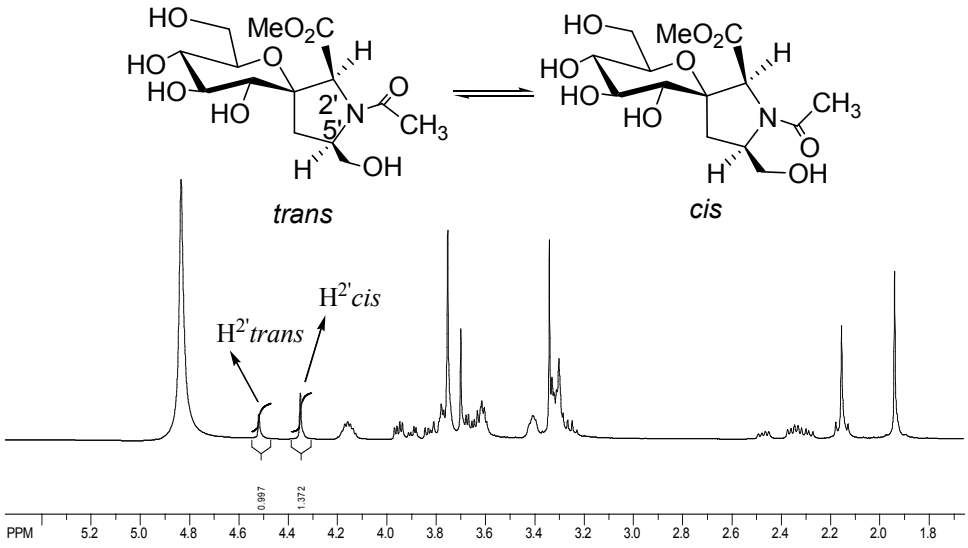

1D nOe spectrum

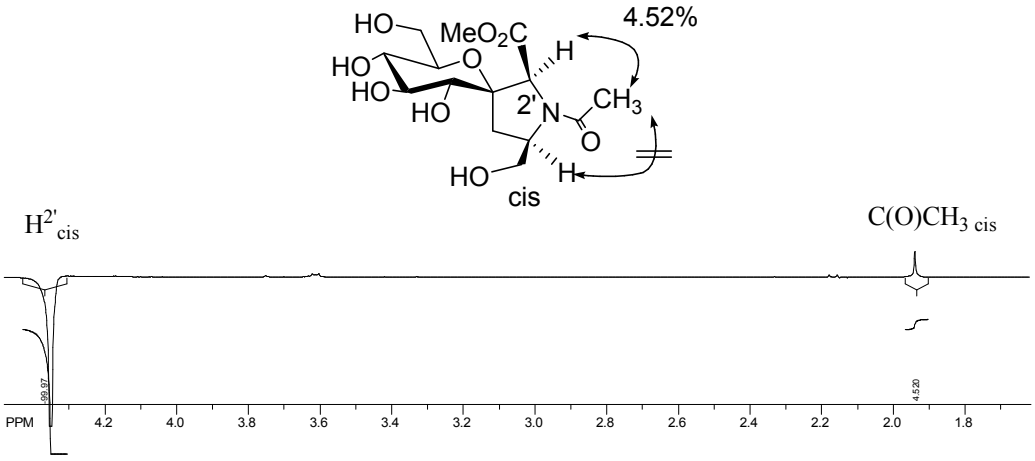

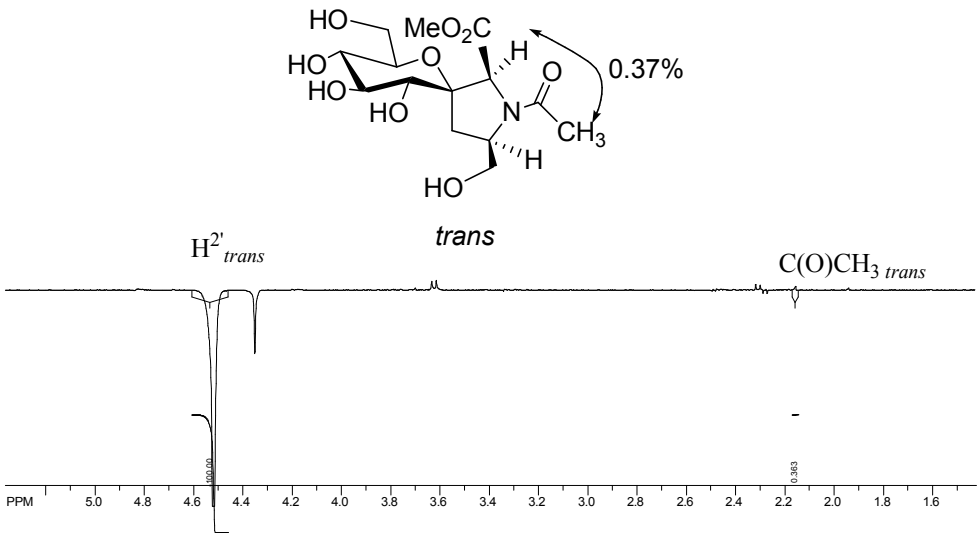

Different chemical shift of C-2′ (α-carbon) for *cis* and *trans* rotamers of compound **4** in CD_3OD (HSQC)

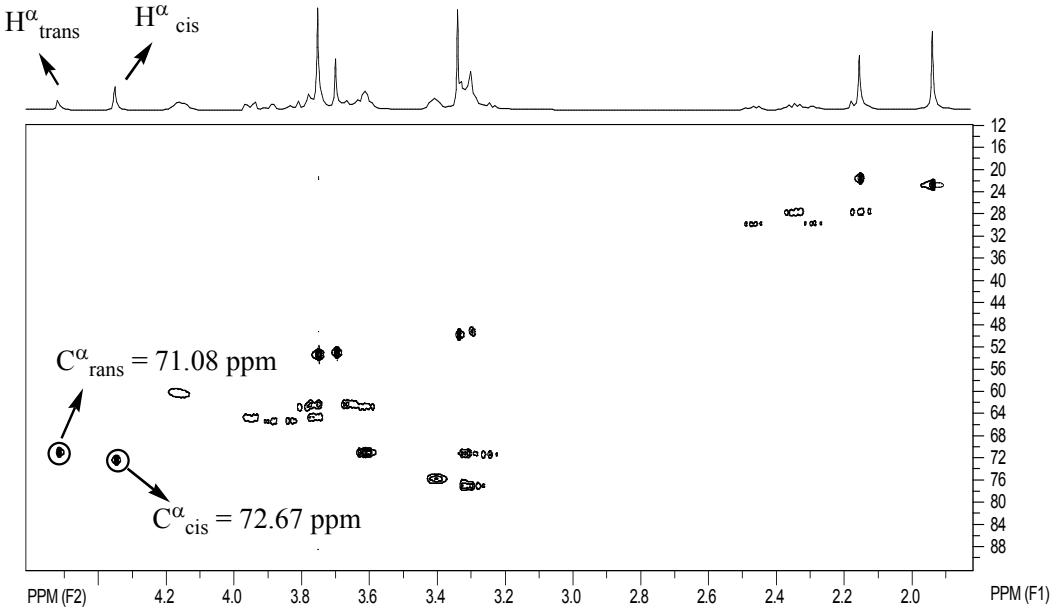

Compound **4** in D_2O

1D nOe spectrum

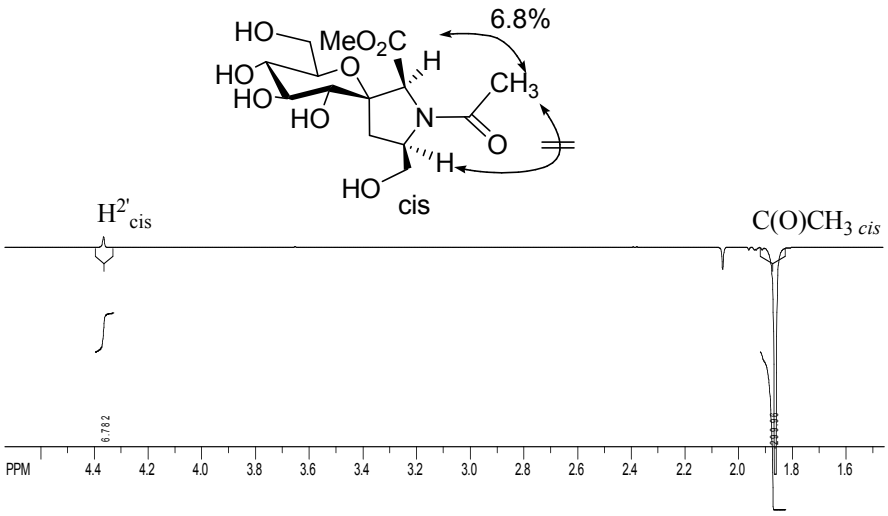

Different chemical shift of C-2′ (α-carbon) for *cis* and *trans* rotamers of compound **4** in D_2O (HSQC)

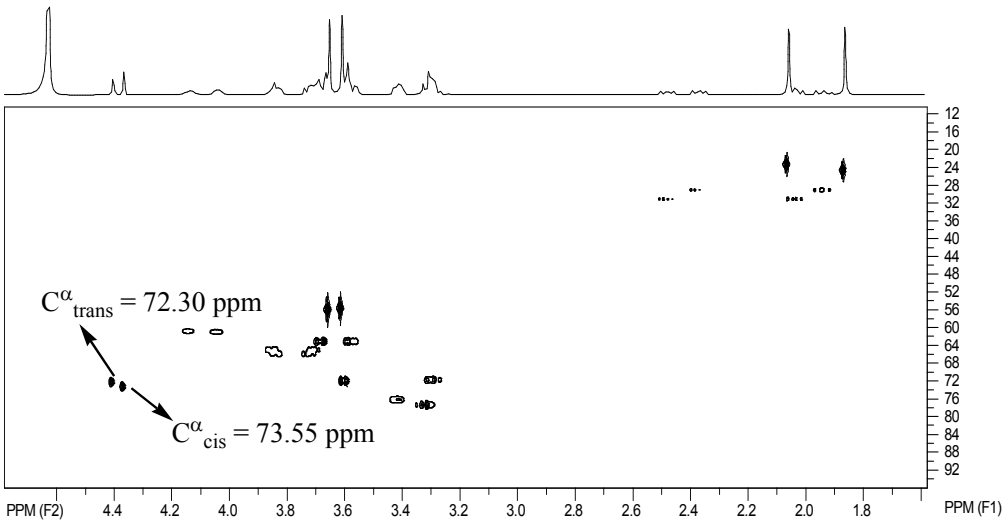

Different chemical shift of α-carbon for *cis* and *trans* rotamers of compound **5** in D_2O (HSQC)

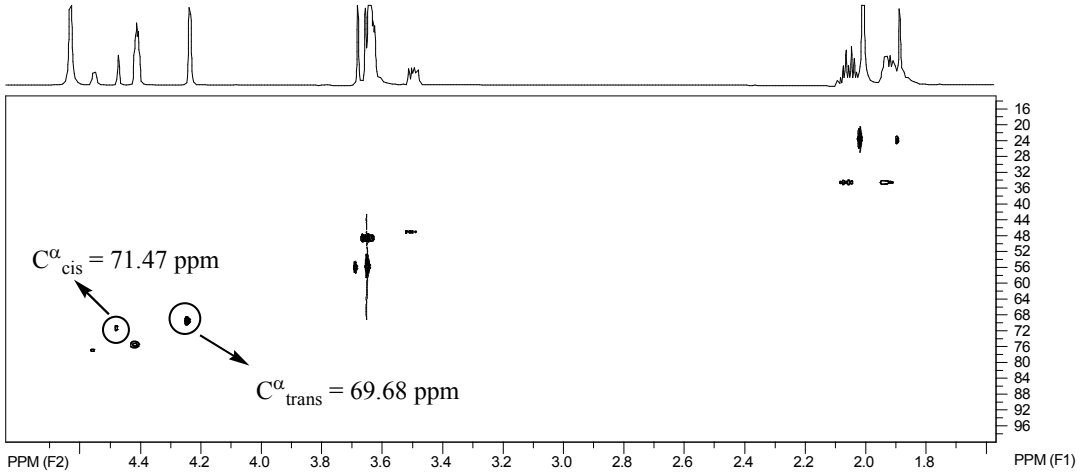

Different chemical shift of α-carbon for *cis* and *trans* rotamers of compound 6 in D_2O (HSQC)

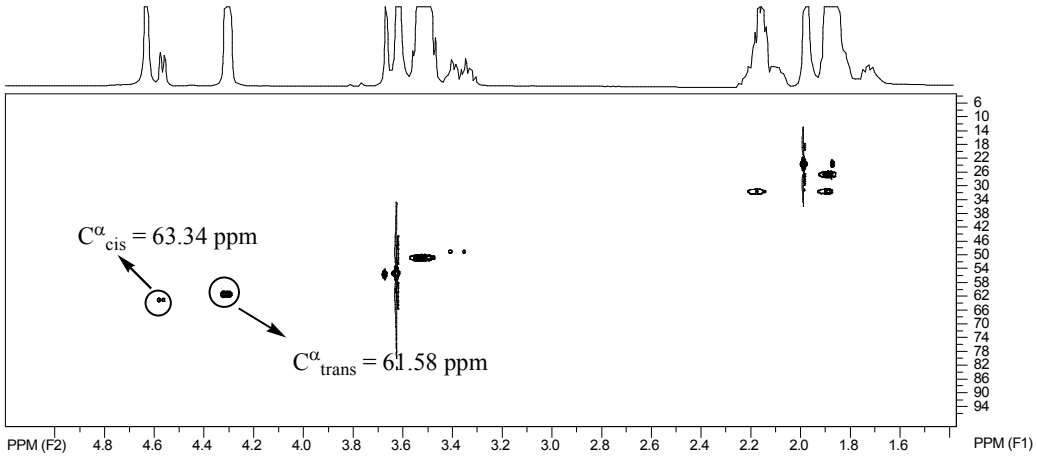

Compound 7 in D_2O

1D nOe spectrum

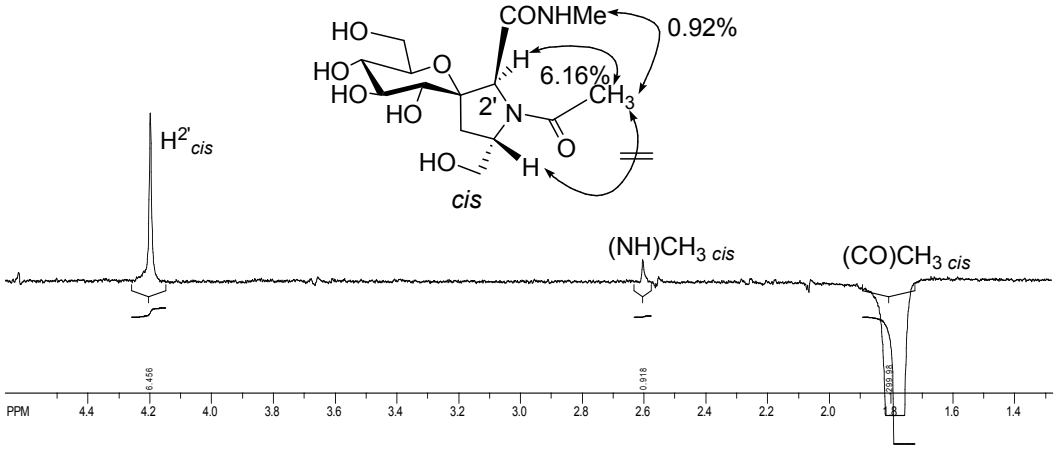

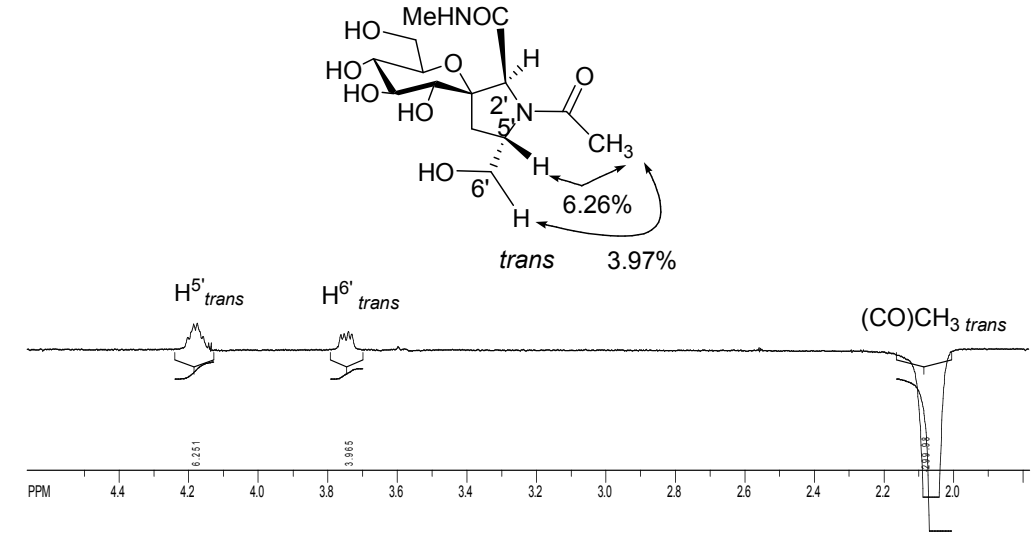

Compound **7** in CD_3OD

1D nOe spectrum

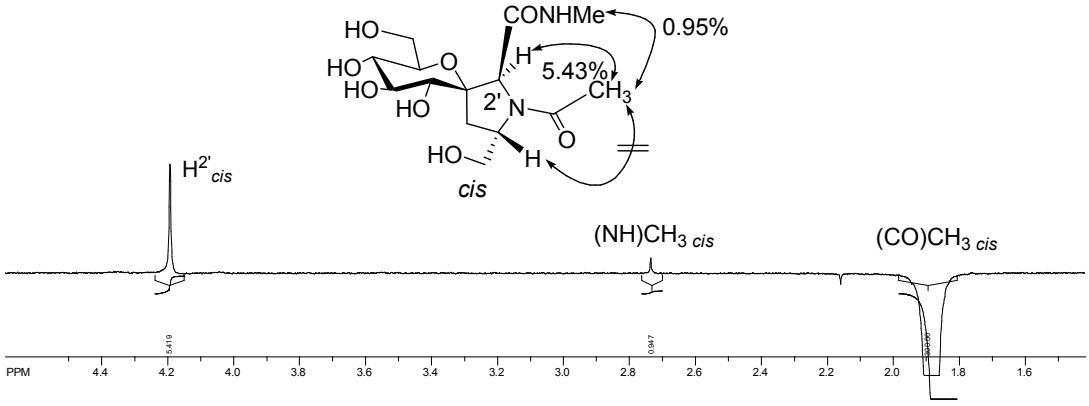

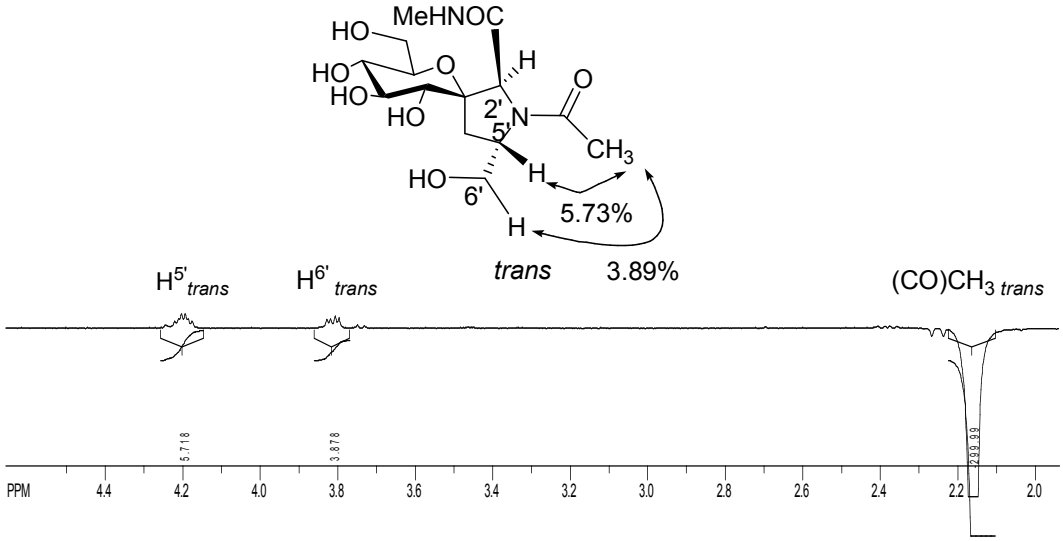

Compound **8** in D_2O

1D nOe spectrum

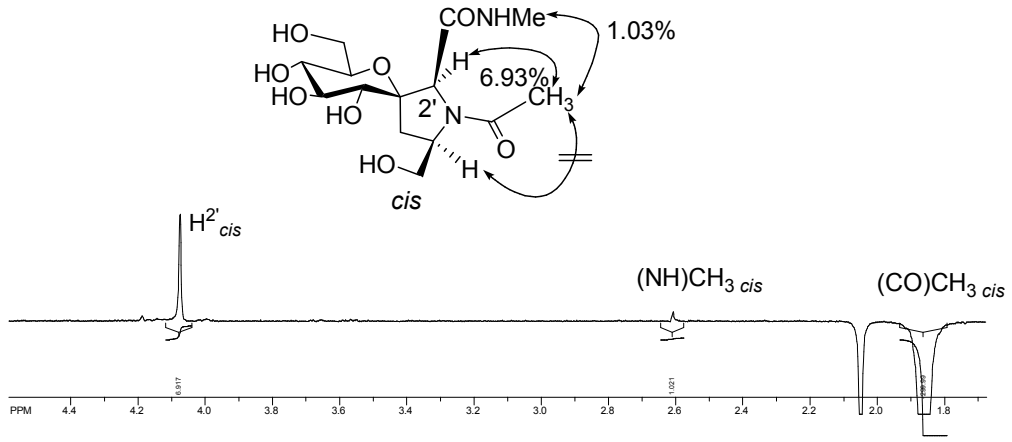

Compound **8** in CD_3OD

1D nOe spectrum

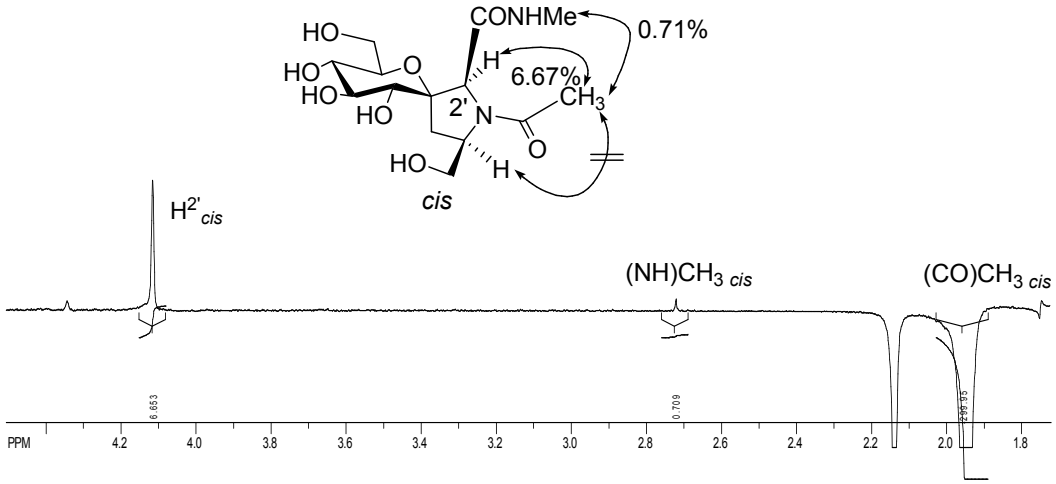

Magnetization transfer NMR experiments were performed on a 500MHz NMR spectrometer, equipped with selective excitation units and a triple resonance (^{1}H, ^{13}C, ^{15}N) gradient inverse probehead. Experiments were performed over several temperatures between 318 and 364 K. Temperature settings of spectrometer were calibrated using an ethylene glycol standard. Selective inversion of proton *trans*- and *cis*-isomer signals were done with Gaussian pulses centered on resonance ±12.5 Hz. Relaxation time was 15 s (**3**), 12 s (**4**), 35 s (**5**) and 40 s (**6**). The inversion-recovery delay of between 1 ms and relaxation time was used. Data for each inversion recovery point were averaged over 32 points. Samples of **3-6** were prepared at concentration of 0.01 M in D_2O. Here, selective inversion of the protons for each compound was different due to their different well-resolved ^{1}H peaks. i.e. The methyl group of prolyl amide (*trans*) for compound **3**, the axil H^{γ} (*cis*) for compound **4**, α-proton for compound **5** and **6** were selectively inversed. ^{1}H NMR spectroscopy was used in preference to ^{13}C NMR since over the course of an experiment, the signal/noise ratio is much higher for ^{1}H than ^{13}C, and heating effects caused by decoupling for ^{13}C causes uncertainty in the temperature of the sample.

The time-dependent magnetization transfers of the *cis* ($M_c(t)$) and *trans* ($M_t(t)$) NMR signals as a function of the inversion transfer time (t) were simultaneously fit to equations 1 and 2 (Alger and Prestegard, 1977; Mariappan and Rabenstein, 1992) below for compounds **3-6** using *Mathematica* (v. 5.0). In the following pulse sequence, the ^{1}H one isomer resonance such as *trans* is selectively inverted using a shaped pulse. Its recovery during t is determined by its intrinsic T_{1t}, magnetization transfer to and from the *cis* resonance, and the T_{1c} of the *cis* resonance:

π(x)sel----------t----------π/2(x,y.-x.-y)---acquire

The resonances of the *trans* and *cis* isomers show the following time dependences:

$$M_t(t) = (c_1)(\tau_t)(\lambda_1+1/\tau_{1c})\exp(\lambda_1 * t) + (c_2)(\tau_2)(\lambda_2+1/\tau_{1c})\exp(\lambda_2 * t) + M_{c\infty} \text{---------- 1}$$

$$M_t(t) = (c_1)\exp(\lambda_1 * t) + (c_2)\exp(\lambda_2 * t) + M_{t\infty} \text{---------- 2}$$

T_{1c} and T_{1t} are the longitudinal relaxation times of the resonances in the absence of exchange.

τ_c and τ_t are the lifetimes of the *cis* and *trans* conformers and k_{ct} and k_{tc} are the corresponding rate constants.

τ_{1c} and τ_{1t} are the effective relaxation times of the *cis* and *trans* resonances when relaxation and exchange are both occurring and are defined below in terms of T_{1c} and τ_c, T_{1t} and τ_t.

λ_1 and λ_2 are related to the time constants τ_c, τ_t, τ_{1c}, and τ_{1t}, and are defined below.

c_1 and c_2 are defined below.

$M_{c\infty}$ and $M_{t\infty}$ are determined experimentally from the magnetization measured after 5 T_1 periods for the *cis* and *trans* resonances, respectively.

Mathematica then calculates τ_t from τ_c, $M_{c\infty}$, and $M_{t\infty}$ as: $\tau_t = \tau_c * Mt_\infty/Mc_\infty$

Thus, $k_{ct} = 1/\tau_c$, $k_{tc} = 1/\tau_t$, $K_{eq} = M_{t\infty}/M_{c\infty}$,$\tau_{1c} = (T_{1c} * \tau_c)/(\tau_c + T_{1c})$, $\tau_{1t} = (T_{1t} * \tau_t)/(\tau_t + T_{1t})$

$\lambda_1 = (0.5)*(-((1/\tau_{1c})+(1/\tau_{1t}))+(((((1/\tau_{1c})+(1/\tau_{1t}))1/2)-(4)*(((1/\tau_{1c})*(1/\tau_{1t}))-((1/\tau c)*(1/\tau t)))))1/2)$

$\lambda_2 = (0.5)*(-((1/\tau_{1c})+(1/\tau_{1t}))-(((((1/\tau_{1c})+(1/\tau_{1t}))2)-(4)*((((1/\tau_{1c}))*((1/\tau_{1t})))-((1/\tau c)*(1/\tau_t)))))1/2)$

$c_2 = ((1/(\tau_t))*(\lambda_1-\lambda_2))*((\tau_t*(\lambda_1+(1/\tau_{1c}))*((M_{0c}-M_{c\infty})+(M_{t\infty}-M_{0t})))$

$c_1 = M_{0c}-M_{c\infty}-c_2$

All experimental data for each compound at different temperature were fit by using Mathematica 5.0 to give the following inversed and inversion-recovery fitting curves:

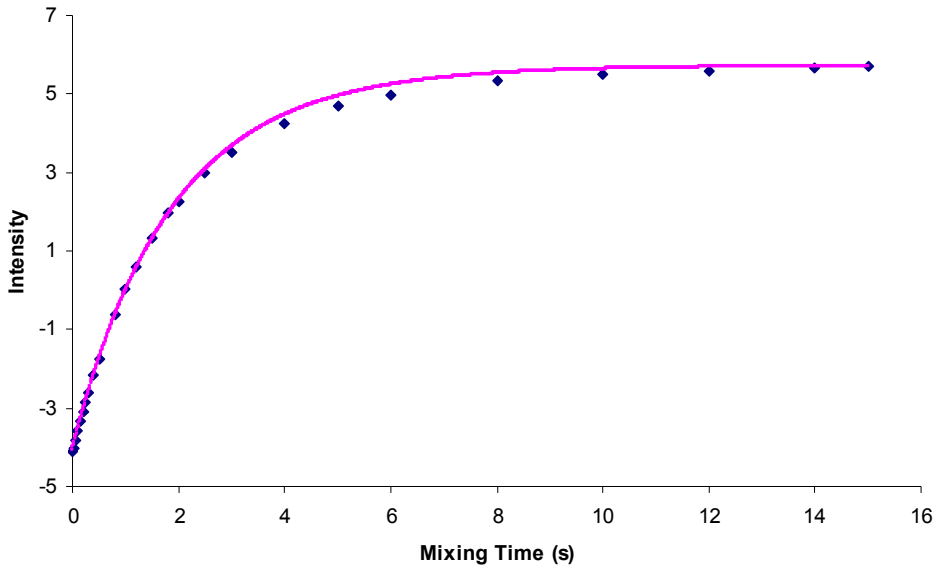

Figure 1. Inversed *N*-amide methyl group (*trans*) for compound **3** at 83°C in D_2O

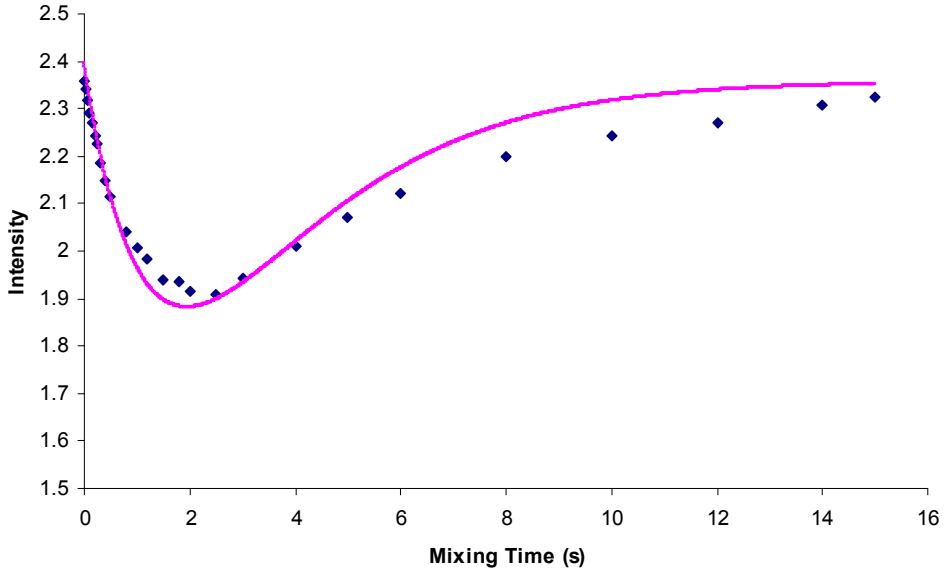

Figure 2. Inversion-recovery of *N*-amide methyl group (*cis*) for compound **3** at 83°C in D_2O

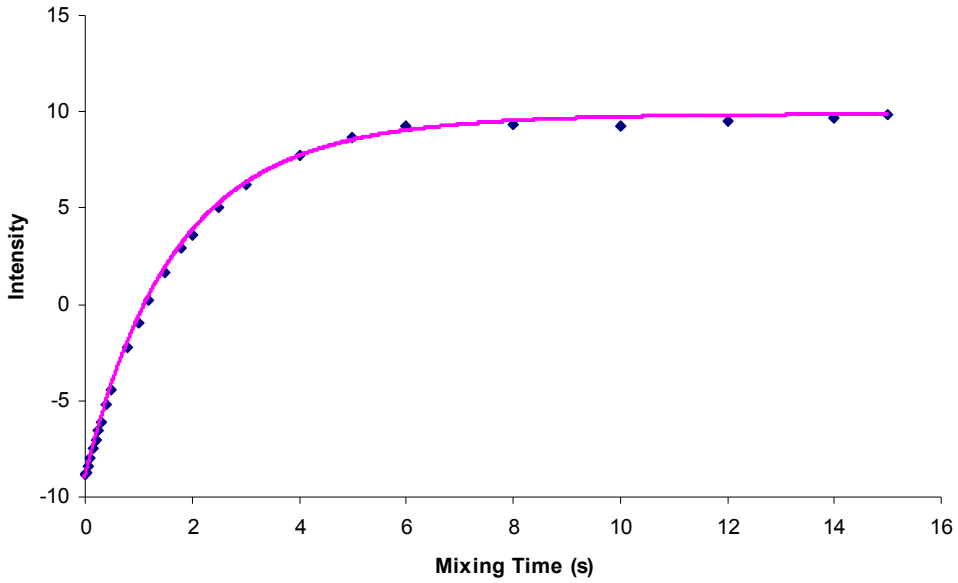

Figure 3. Inversed *N*-amide methyl group (*trans*) for compound **3** at 86°C in D_2O

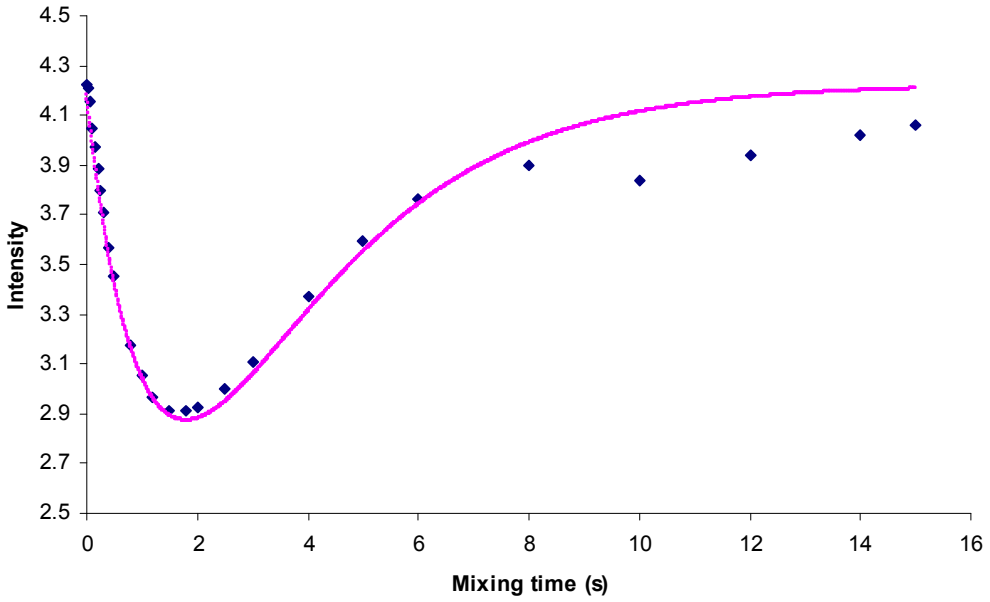

Figure 4. Inversion-recovery of *N*-amide methyl group (*cis*) for compound **3** at 86°C in D_2O

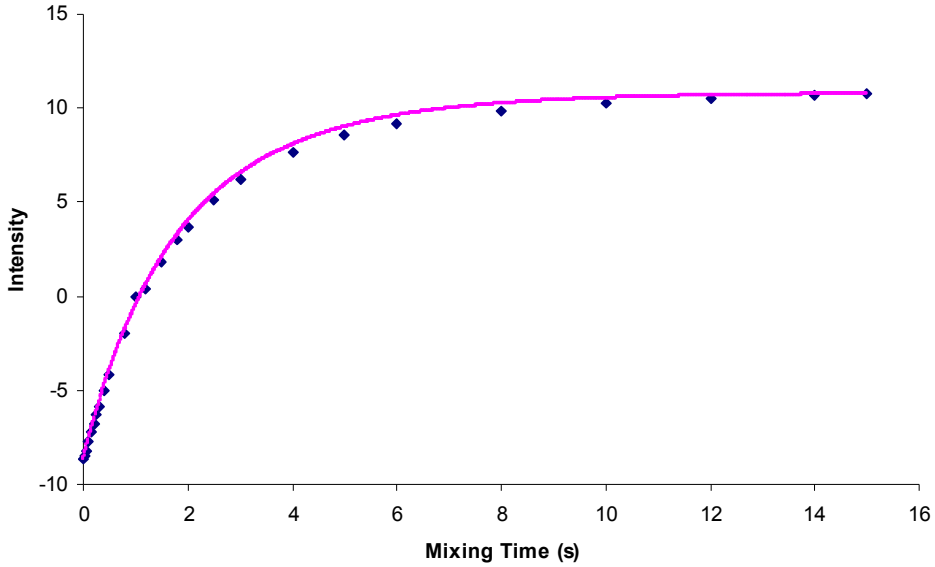

Figure 5. Inversed *N*-amide methyl group (*trans*) for compound **3** at 89°C in D_2O

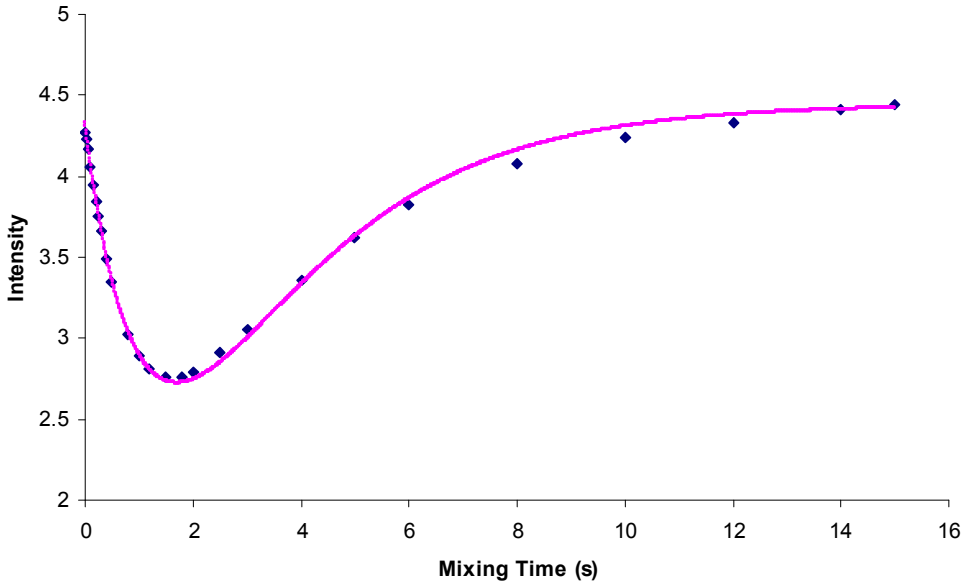

Figure 6. Inversion-recovery of *N*-amide methyl group (*cis*) for compound **3** at 89°C in D_2O

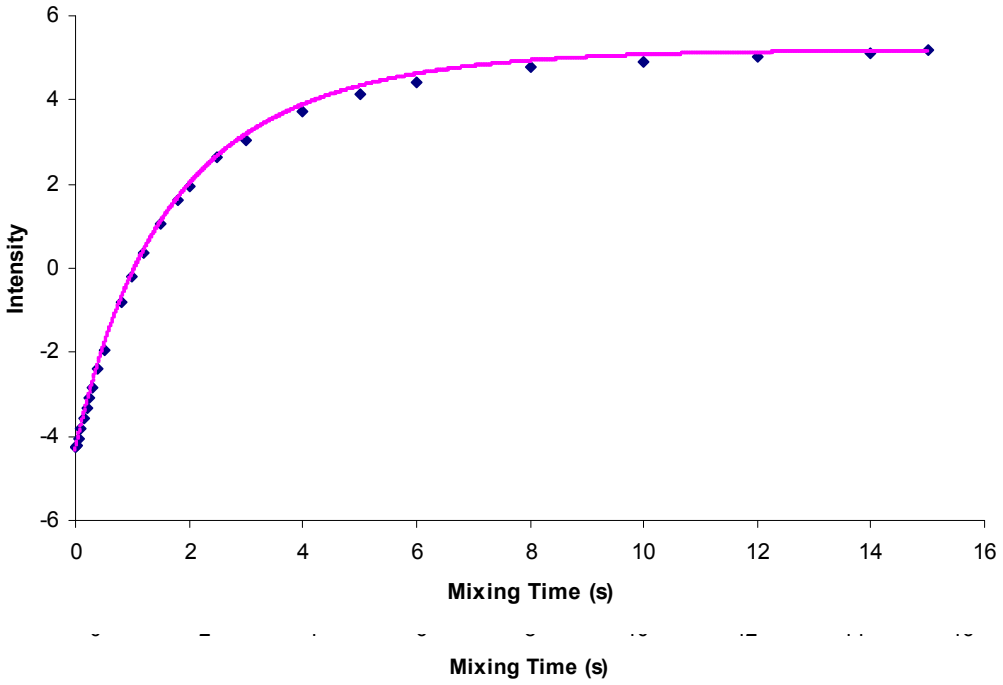

Figure 7. Inversed *N*-amide methyl group (*trans*) for compound **3** at 91°C in D_2O

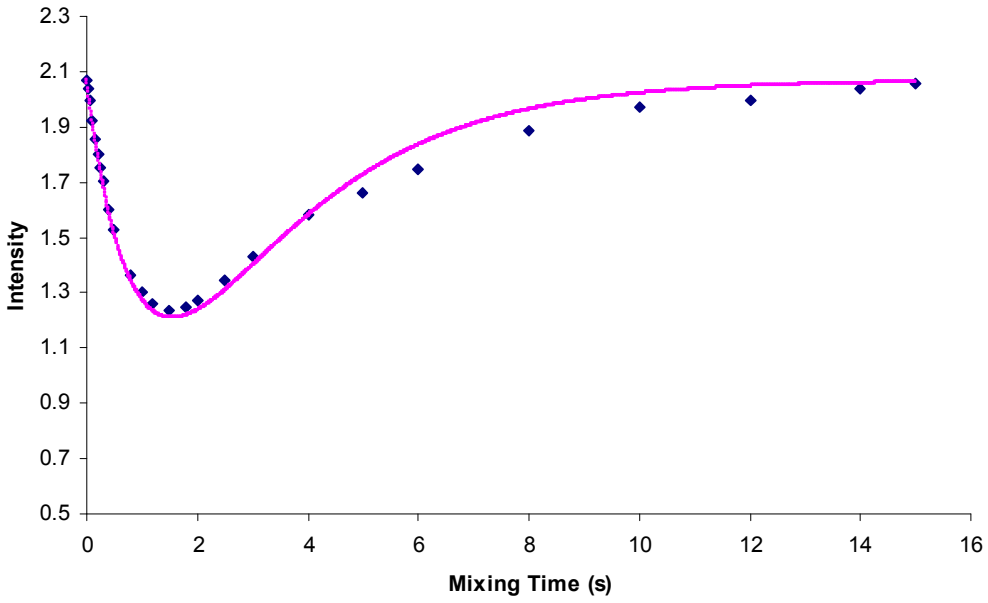

Figure 8. Inversion-recovery of *N*-amide methyl group (*cis*) for compound **3** at 91°C in D_2O

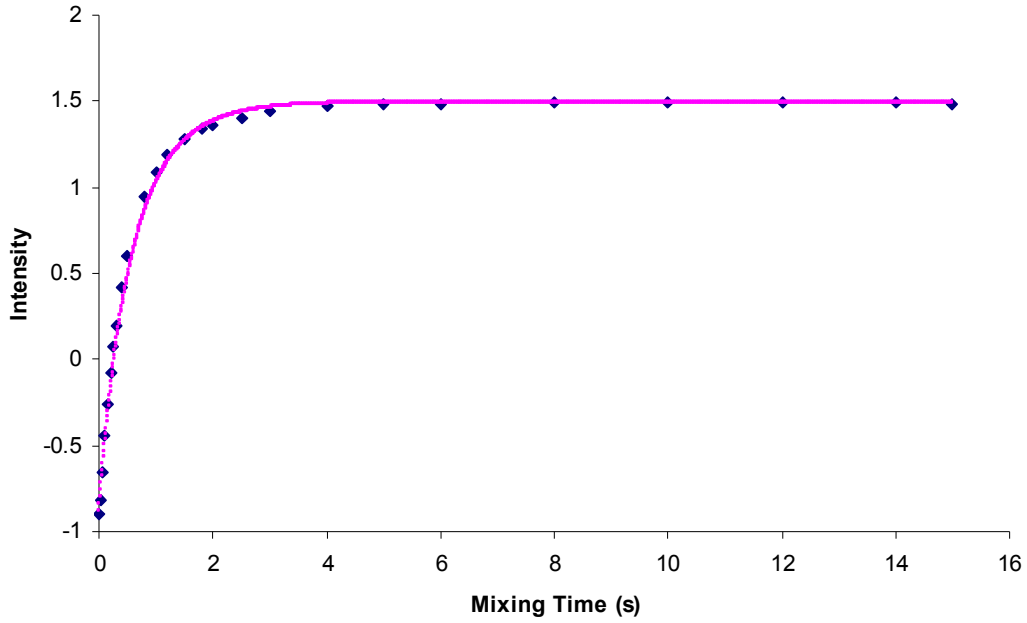

Figure 9. Inversed *N*-amide methyl group (*trans*) for compound **3** at 93°C in D_2O

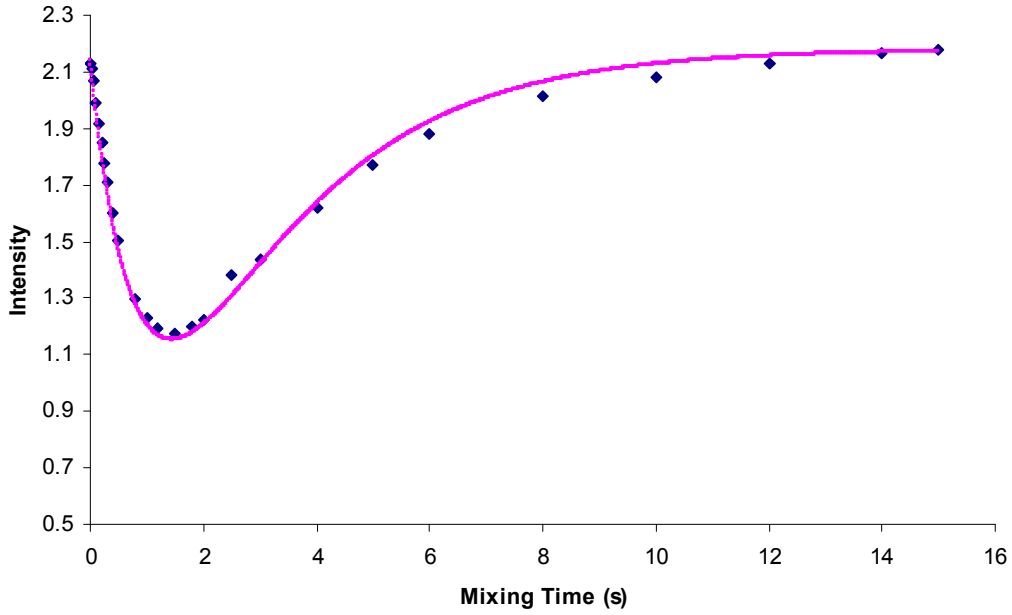

Figure 10. Inversion-recovery of *N*-amide methyl group (*cis*) for compound **3** at 93°C in D_2O

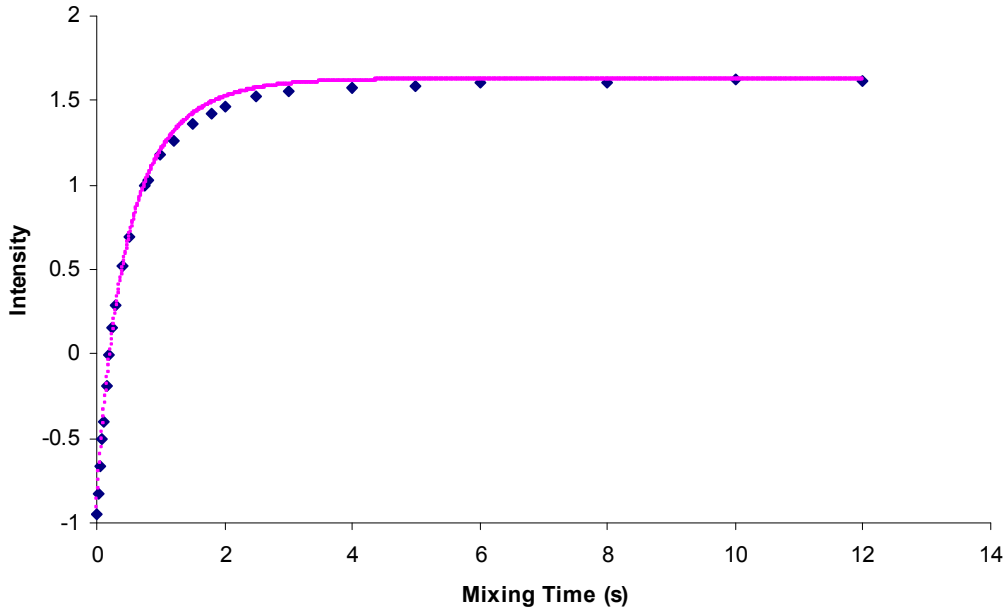

Figure 11. Inversed δ-position axial proton (*cis*) for compound **4** at 46°C in D_2O

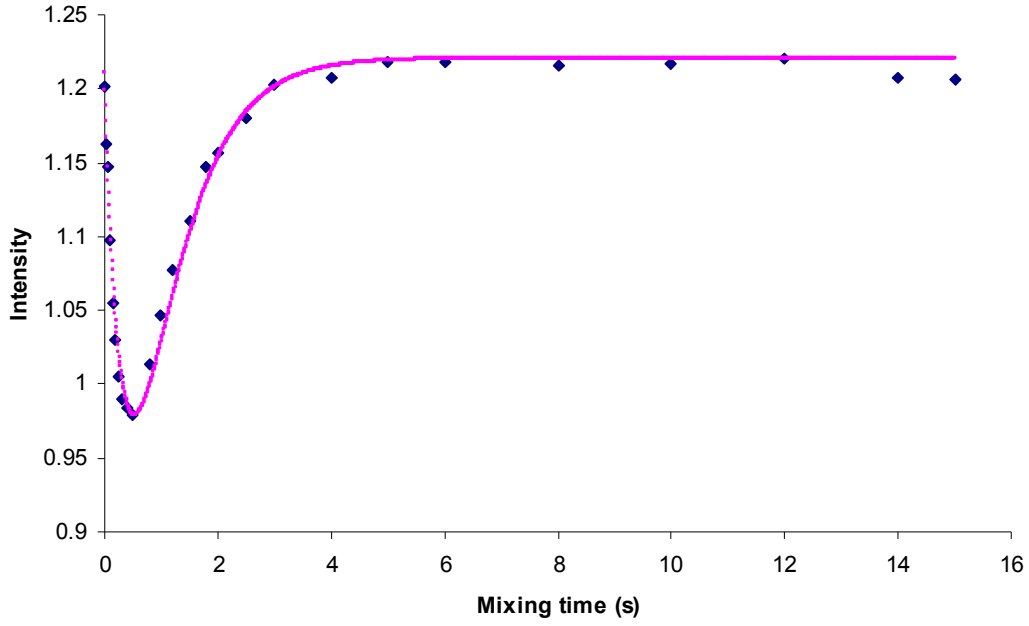

Figure 12. Inversion-recovery of non-inversed δ-position axial proton (*trans*) for compound **4** at 46°C in D_2O

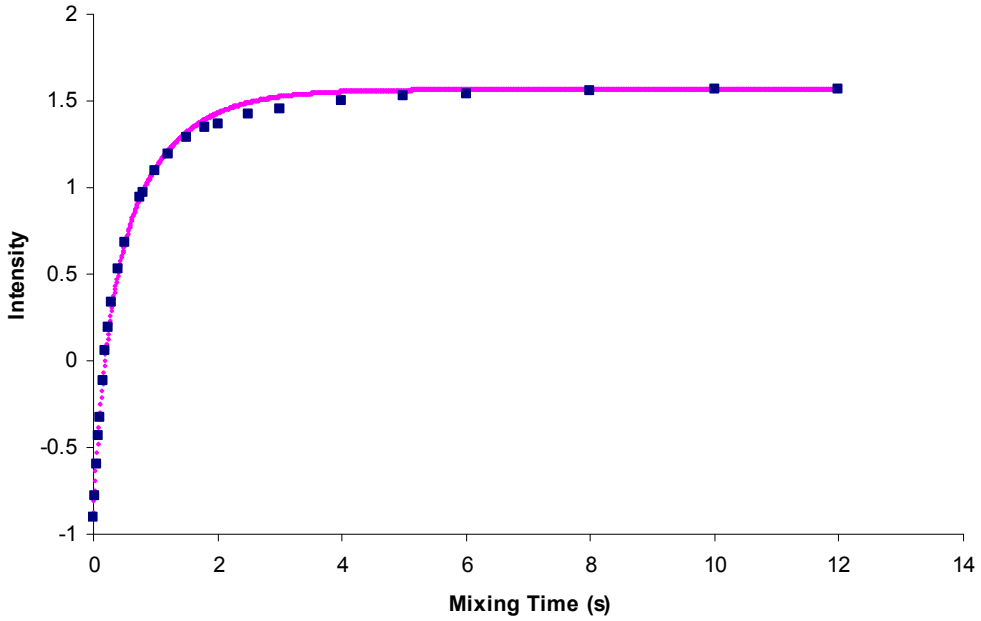

Figure 13. Inversed δ-position axial proton (*cis*) for compound **4** at 52°C in D_2O

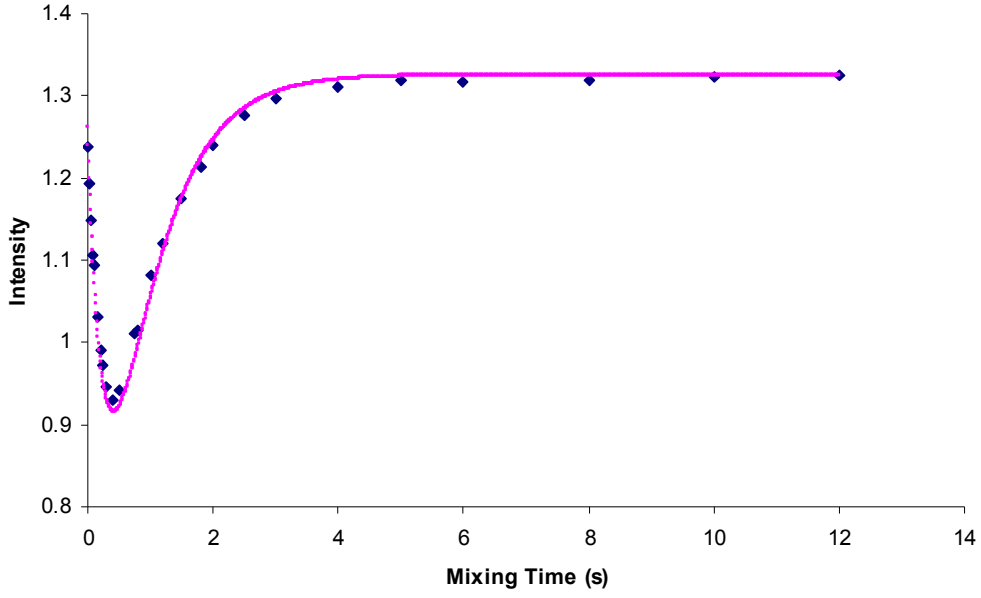

Figure 14. Inversion-recovery of non-inversed δ-position axial proton (*trans*) for compound **4** at 52°C in D_2O

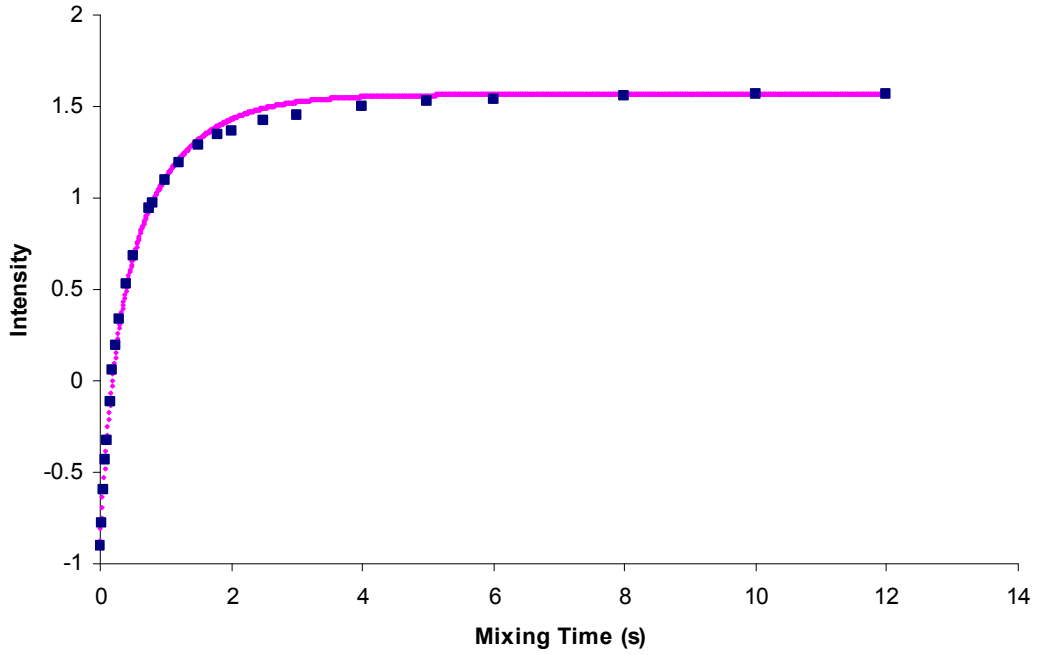

Figure 15. Inversed δ-position axial proton (*cis*) for compound **4** at 57°C in D_2O

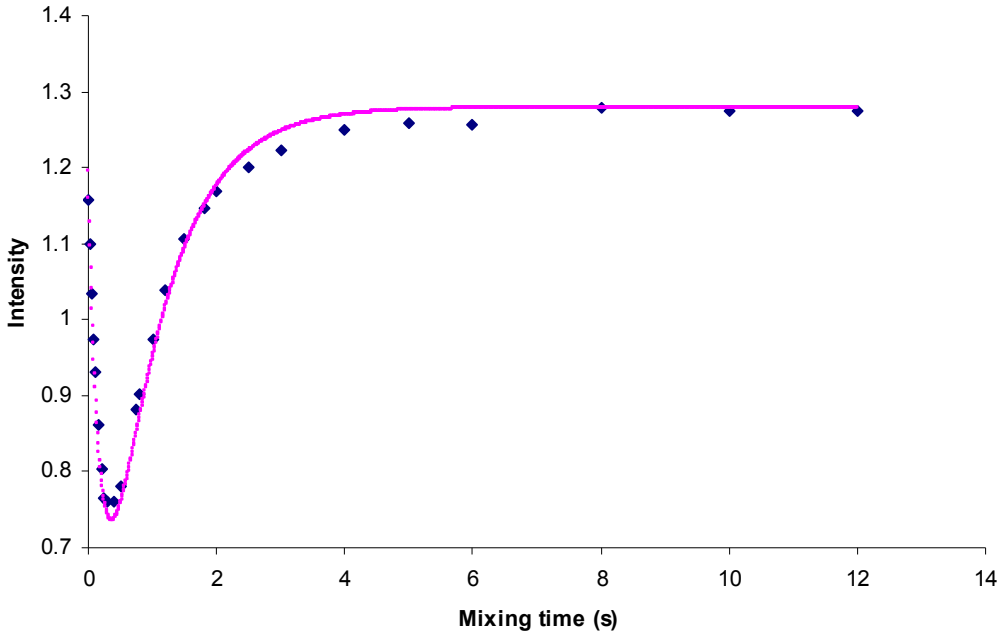

Figure 16. Inversion-recovery of non-inversed δ-position axial proton (*trans*) for compound **4** at 57°C in D_2O

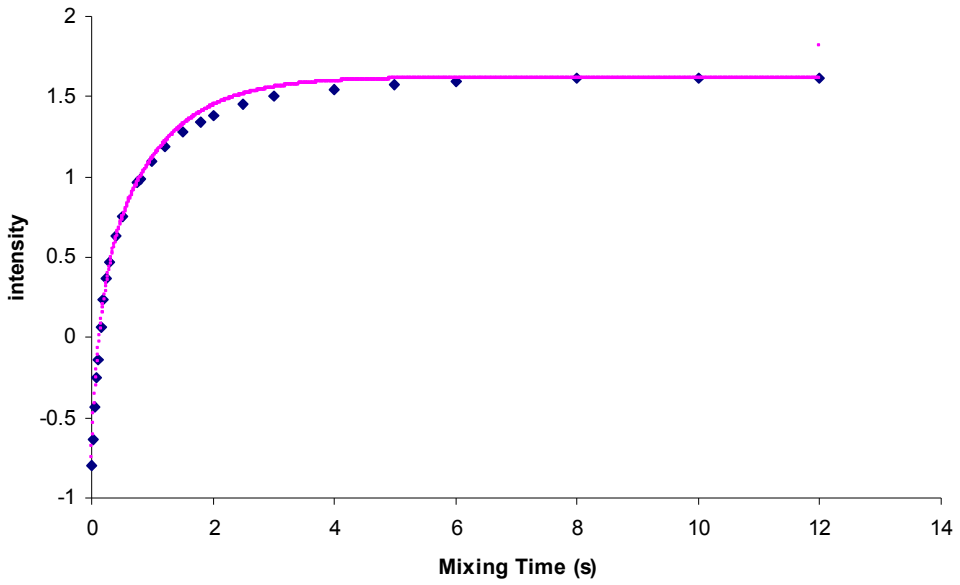

Figure 17. Inversed δ-position axial proton (*cis*) for compound **4** at 62°C in D_2O

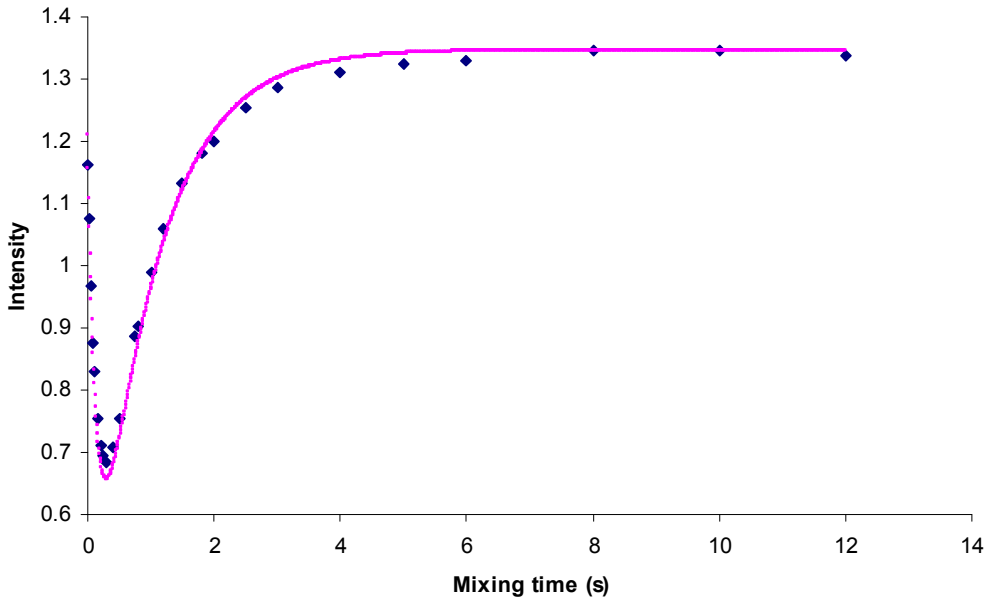

Figure 18. Inversion-recovery of non-inversed δ-position axial proton (*trans*) for compound **4** at 62°C in D_2O

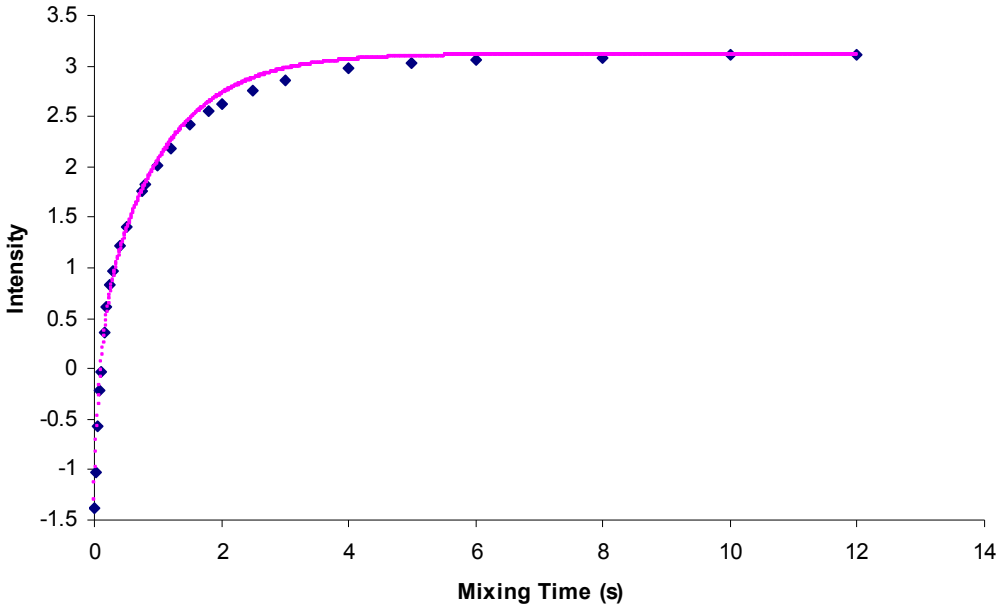

Figure 19. Inversed δ-position axial proton (*cis*) for compound **4** at 67°C in D_2O

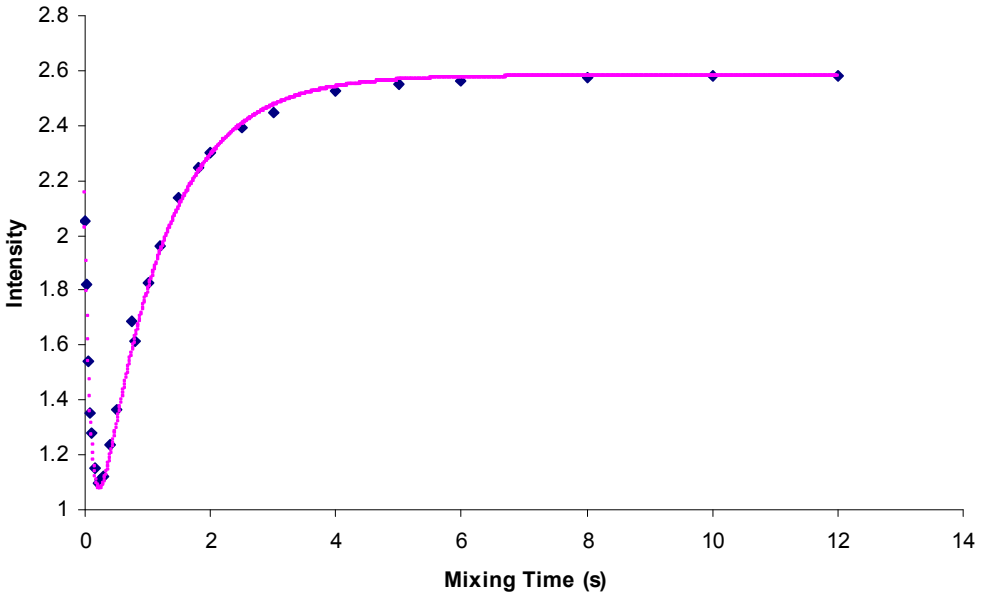

Figure 20. Inversion-recovery of non-inversed δ-position axial proton (*trans*) for compound **4** at 67°C in D_2O

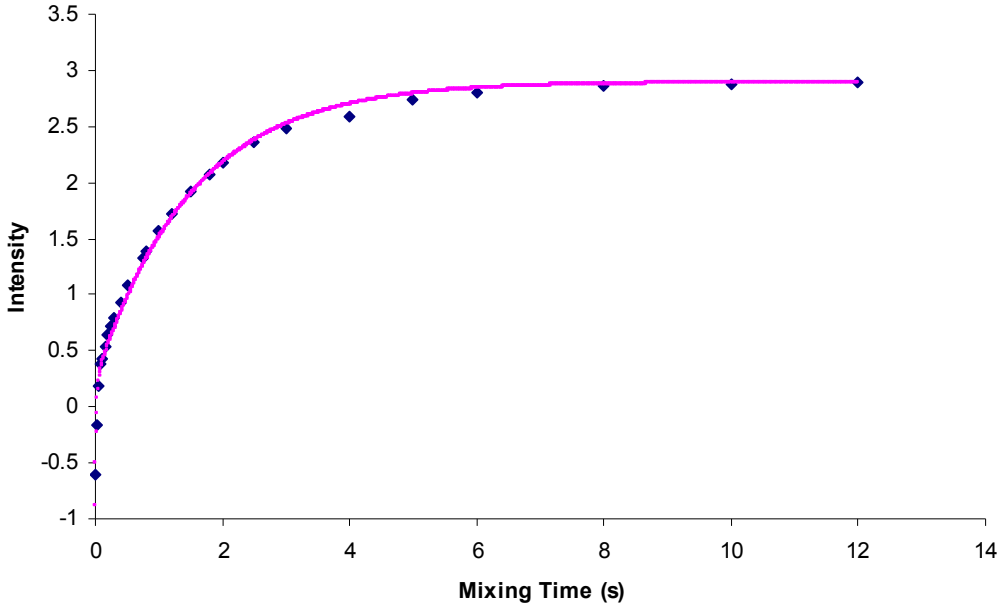

Figure 21. Inversed δ-position axial proton (*cis*) for compound **4** at 83°C in D_2O

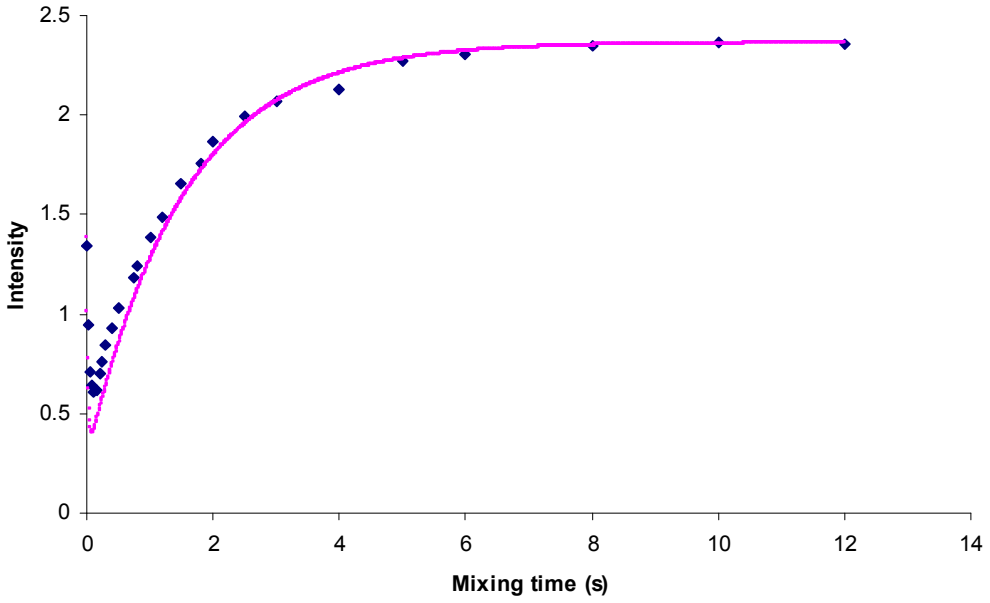

Figure 22. Inversion-recovery of non-inversed δ-position axial proton (*trans*) for compound **4** at 83°C in D_2O

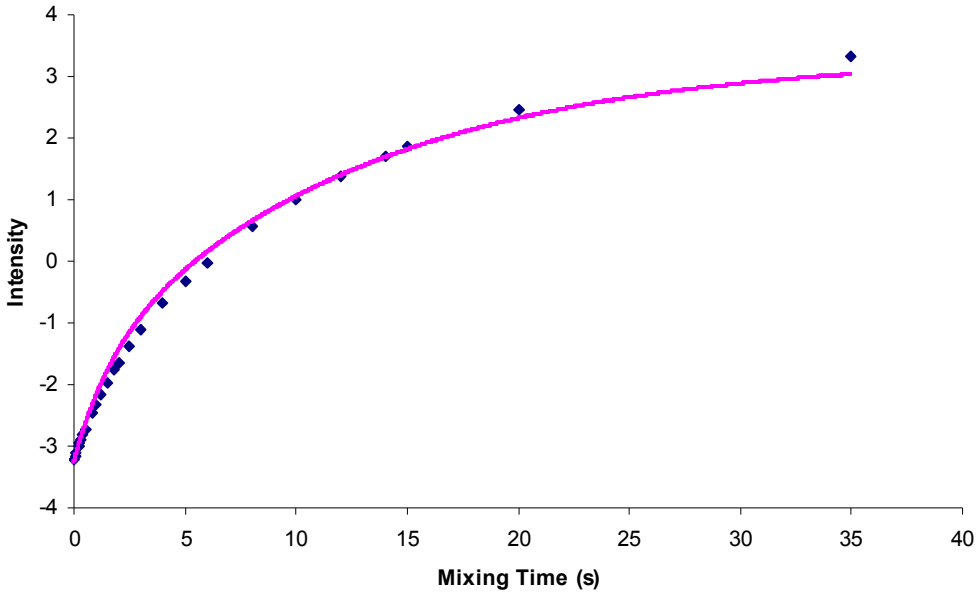

Figure 23. Inversed α-proton (*trans*) for compound **5** at 62°C in D_2O

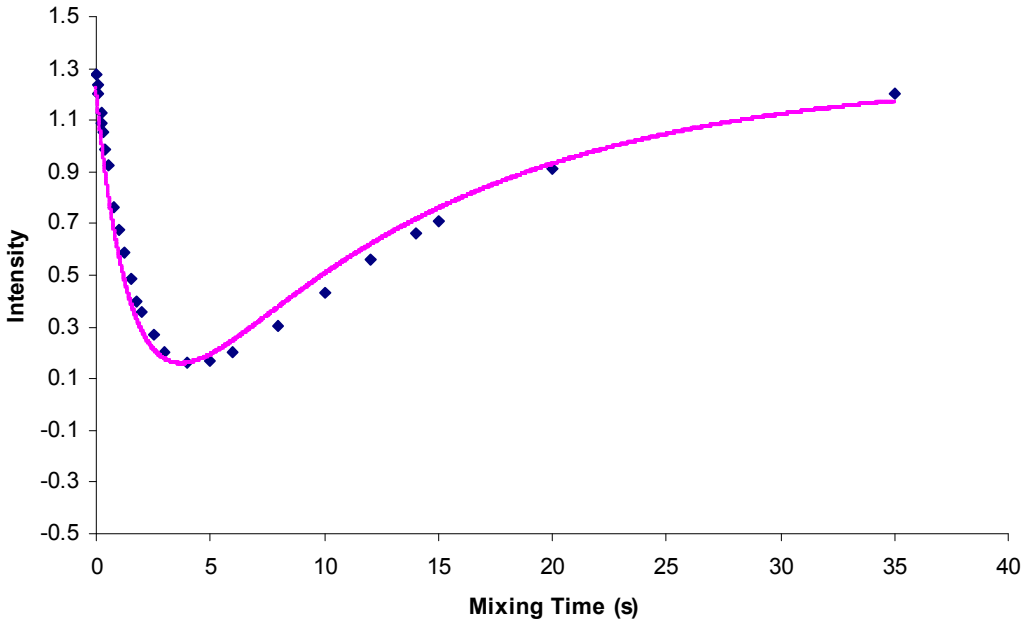

Figure 24. Inversion-recovery of α-proton (*cis*) for compound **5** at 62°C in D_2O

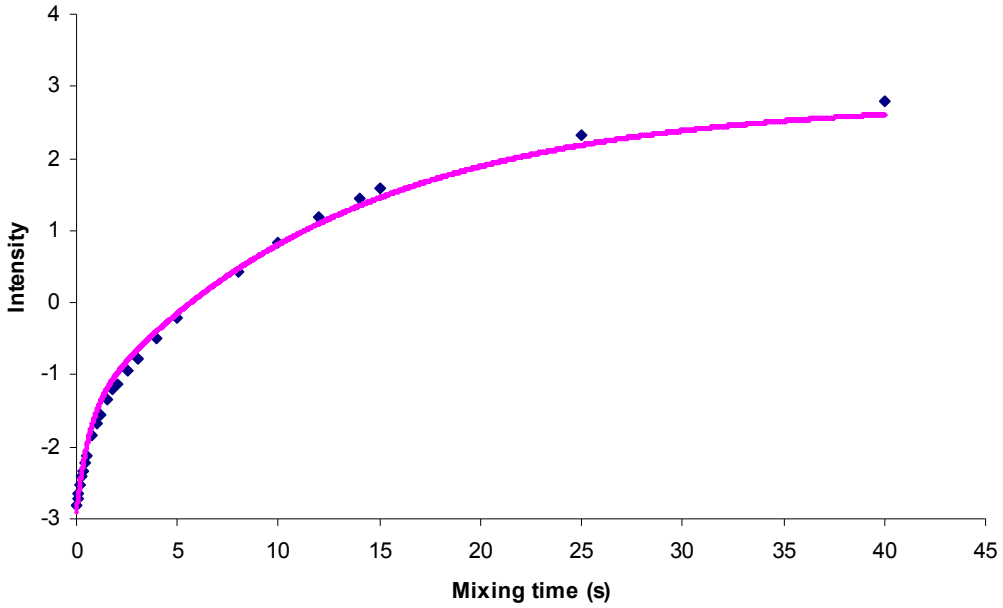

Figure 25. Inversed α-proton (*trans*) for compound **5** at 73°C in D_2O

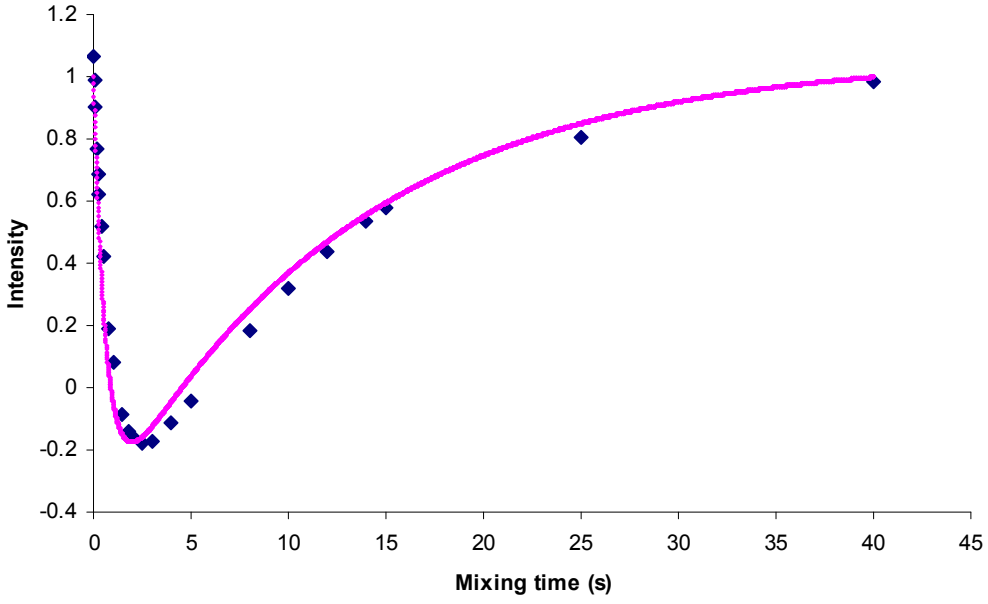

Figure 26. Inversed-recovery α-proton (*cis*) for compound **5** at 73°C in D_2O

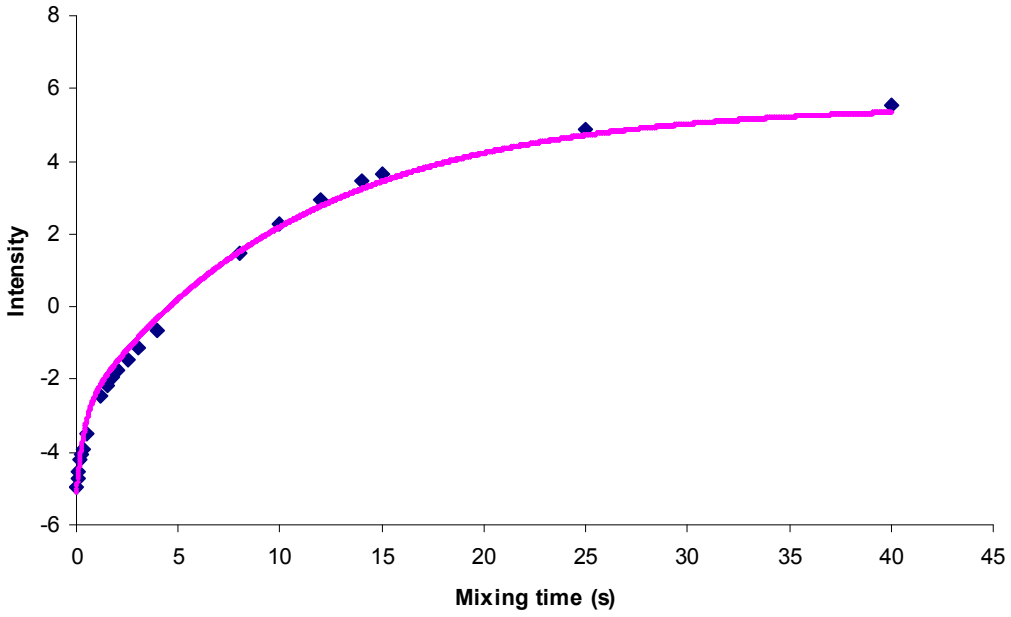

Figure 27. Inversed α-proton (*trans*) for compound **5** at 78°C in D_2O

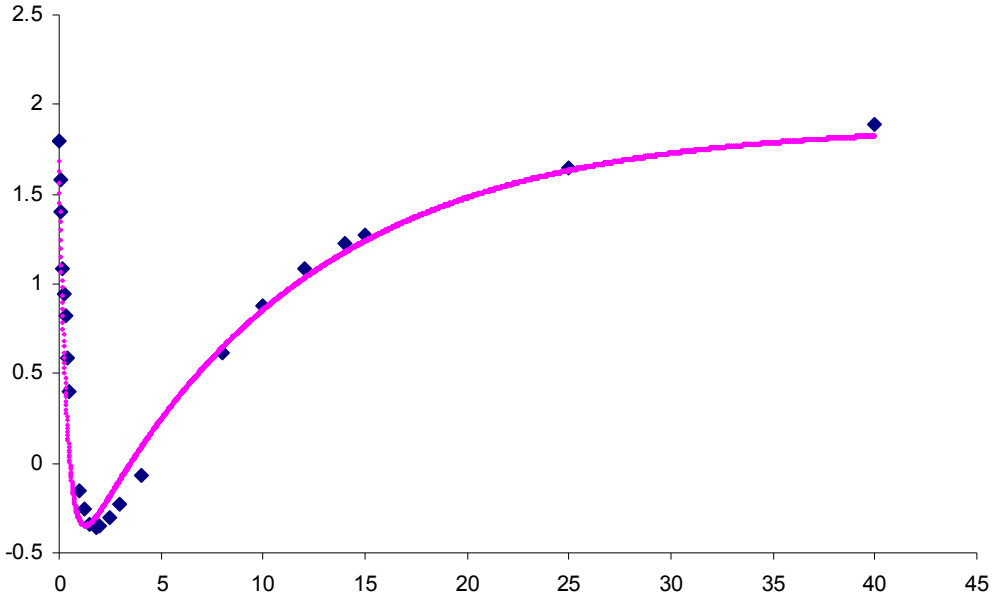

Figure 28. Inversed-recovery α-proton (*cis*) for compound **5** at 78°C in D_2O

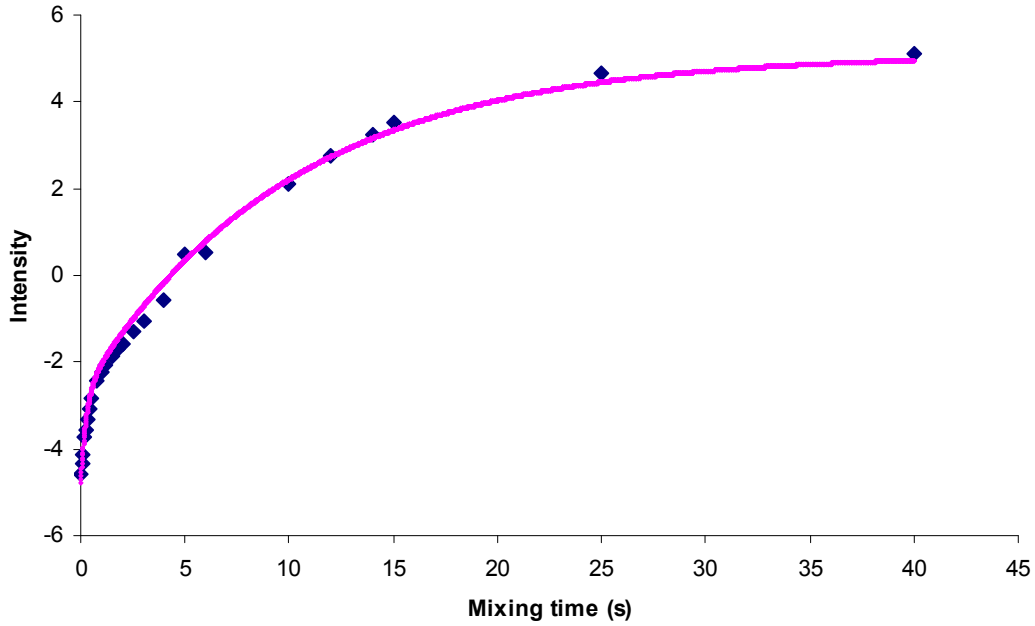

Figure 29. Inversed α-proton (*trans*) for compound **5** at 83°C in D_2O

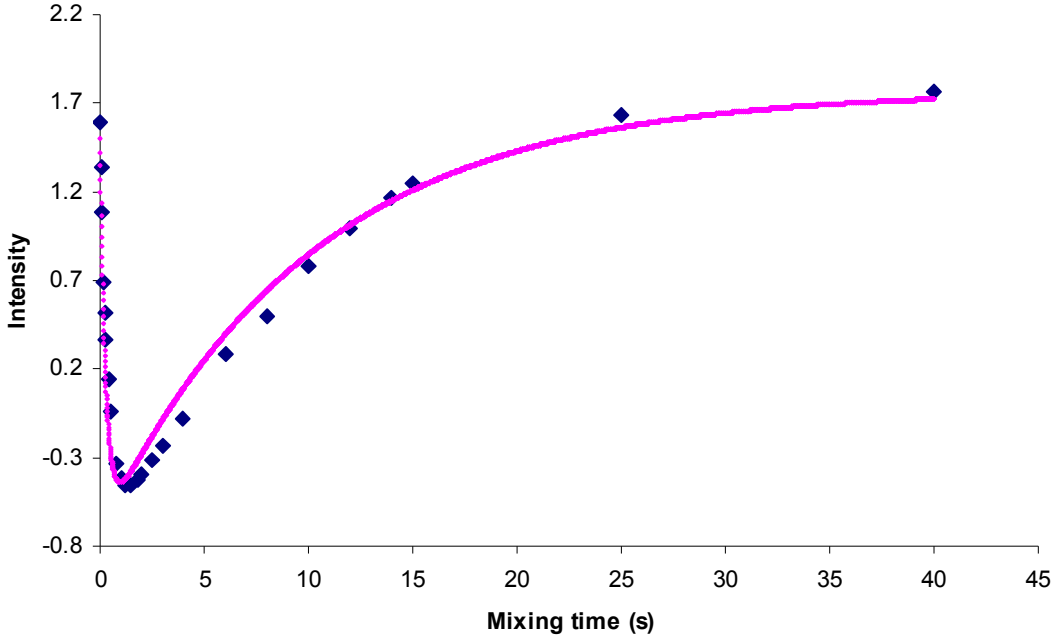

Figure 30. Inversed-recovery α-proton (*trans*) for compound **5** at 83°C in D_2O

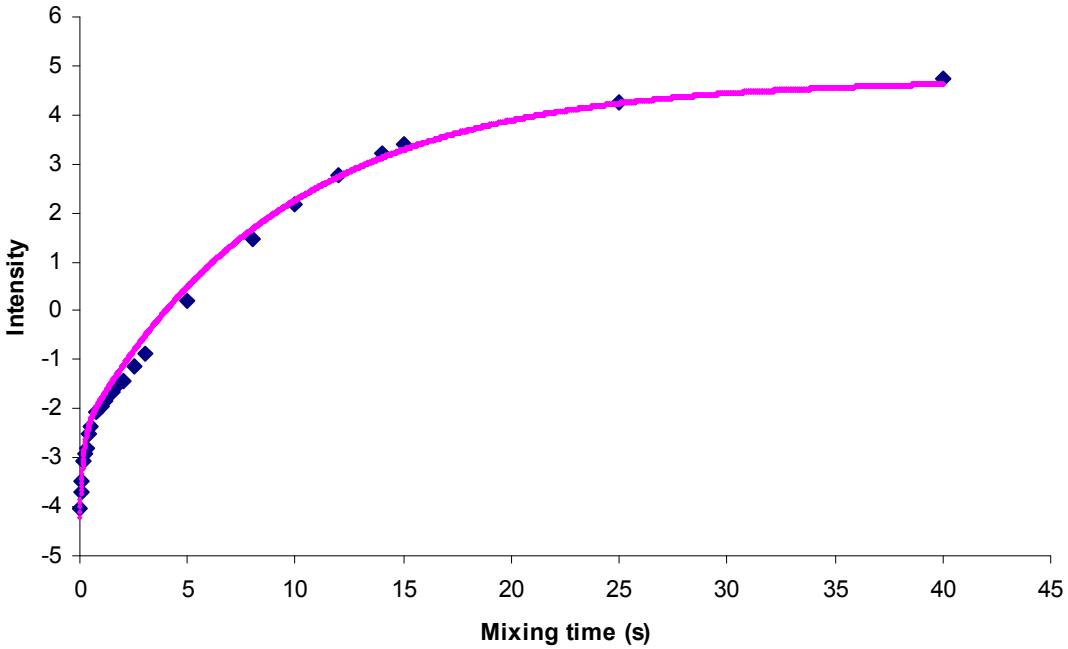

Figure 31. Inversed α-proton (*cis*) for compound **5** at 89°C in D_2O

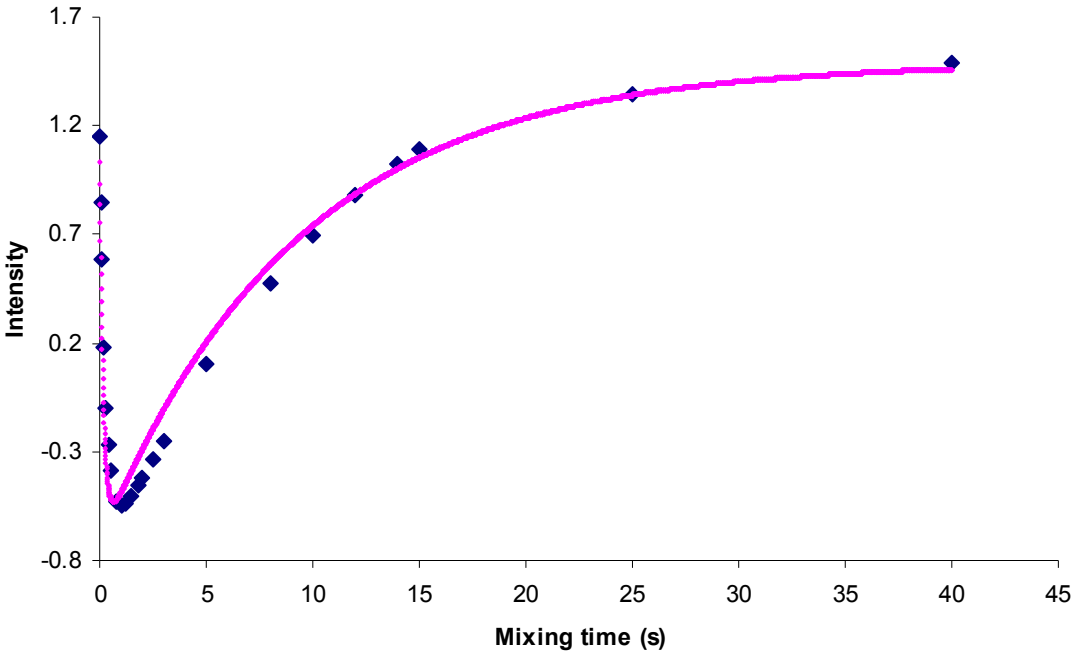

Figure 32. Inversed–recovery α-proton (*trans*) for compound **5** at 89°C in D_2O

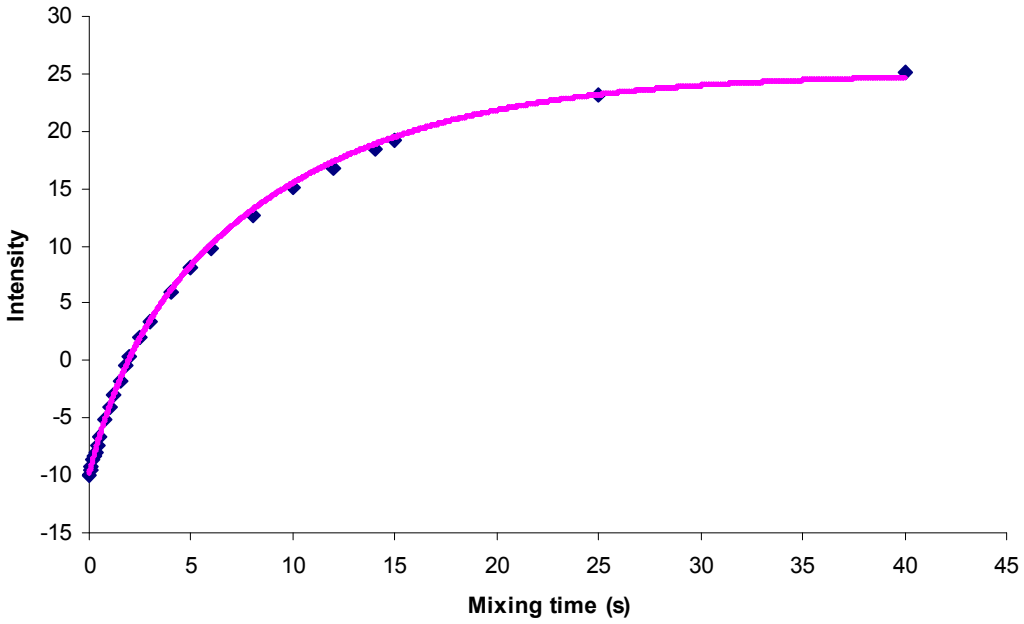

Figure 33. Inversed α-proton (*trans*) for compound **6** at 62°C in D_2O

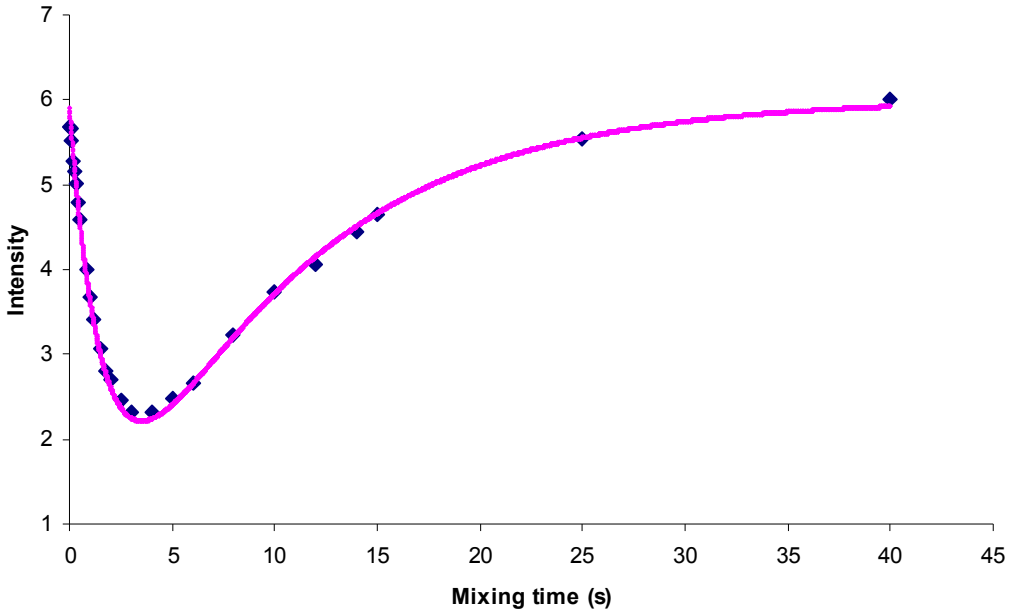

Figure 34. Inversed-recovery α-proton (*cis*) for compound **6** at 62°C in D_2O

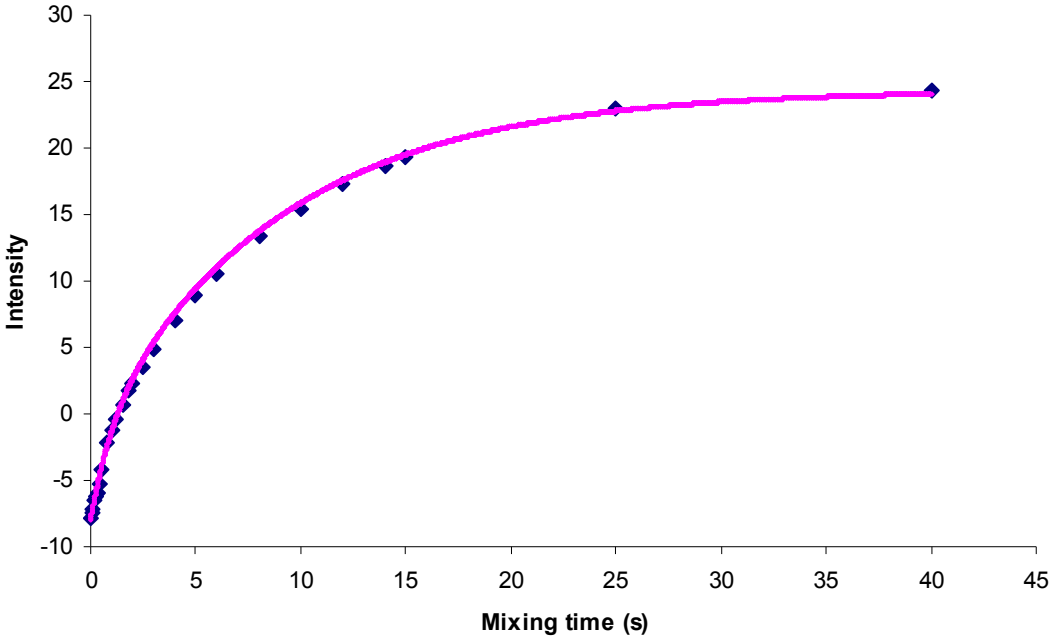

Figure 35. Inversed α-proton (*trans*) for compound **6** at 67°C in D_2O

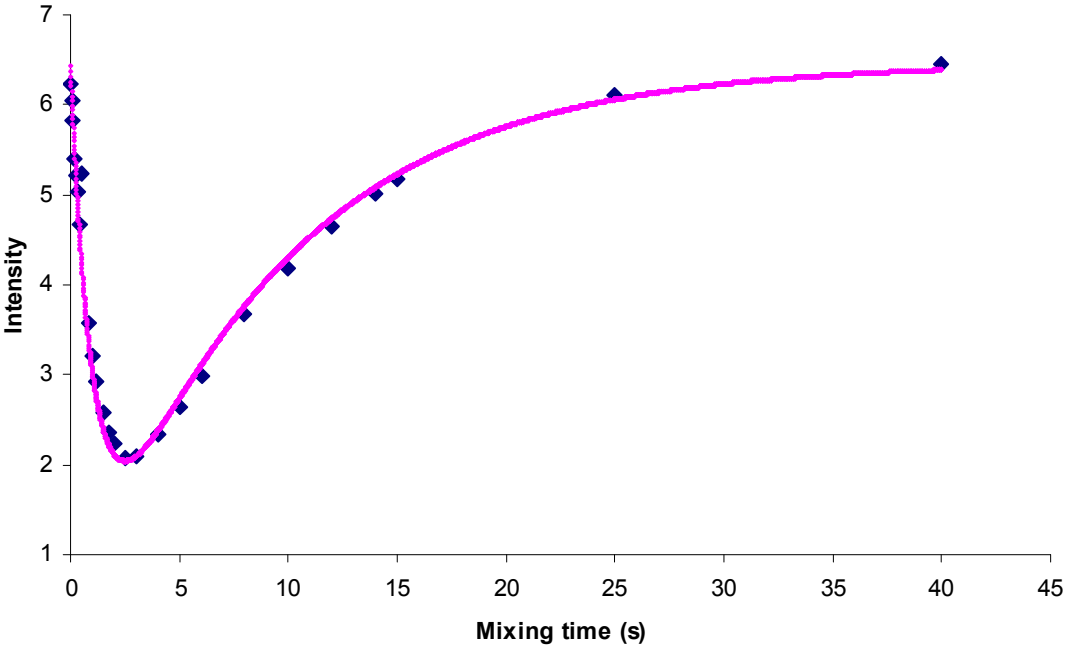

Figure 36. Inversed-recovery α-proton (*cis*) for compound **6** at 67°C in D_2O

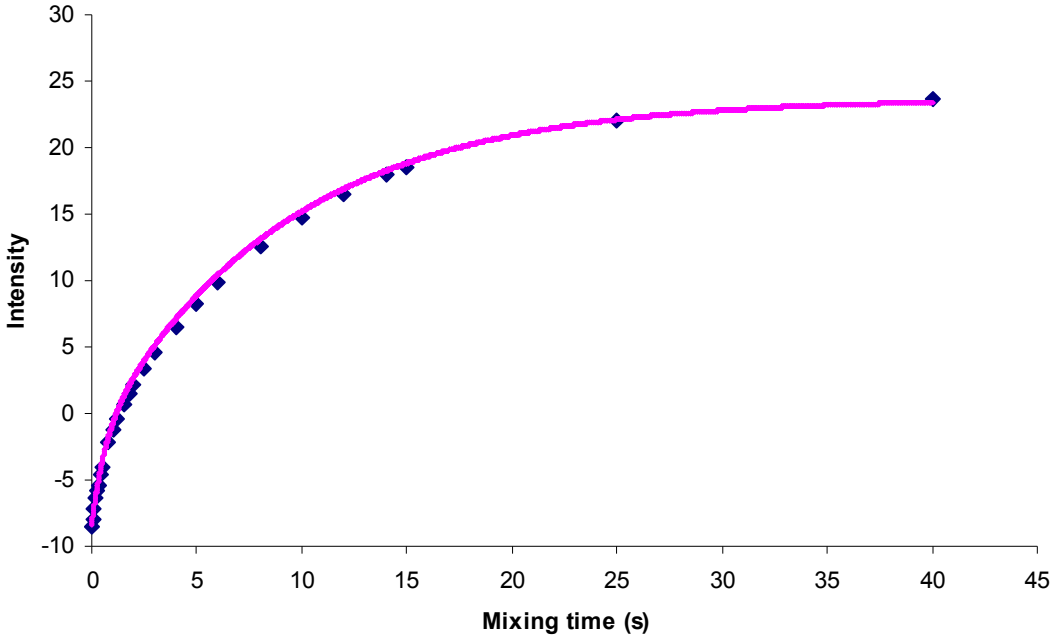

Figure 37. Inversed α-proton (*trans*) for compound **6** at 73°C in D_2O

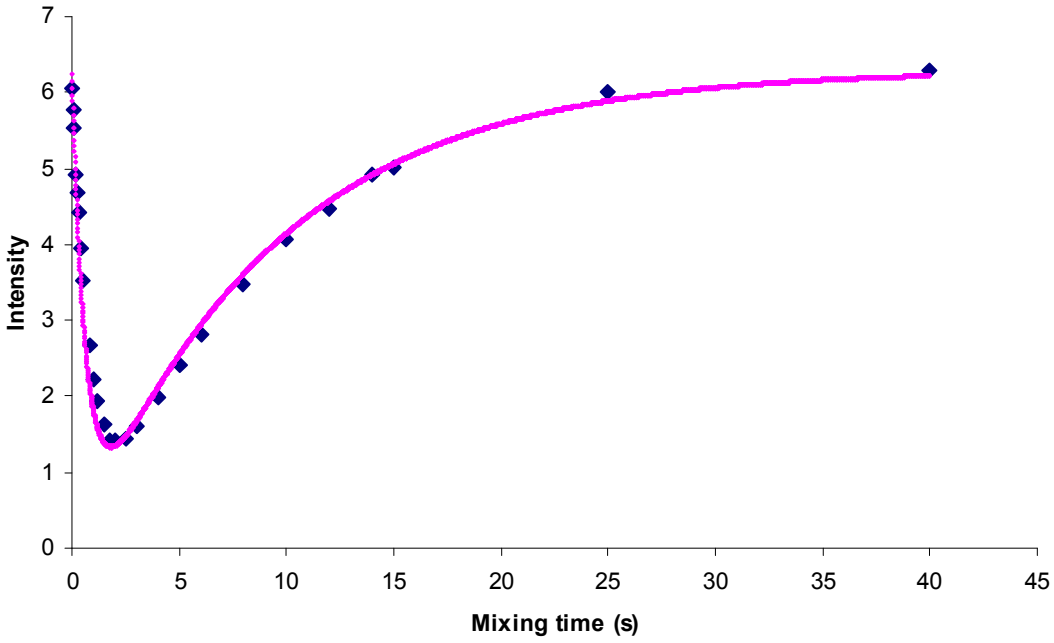

Figure 38. Inversed-recovery α-proton (*cis*) for compound **6** at 73°C in D_2O

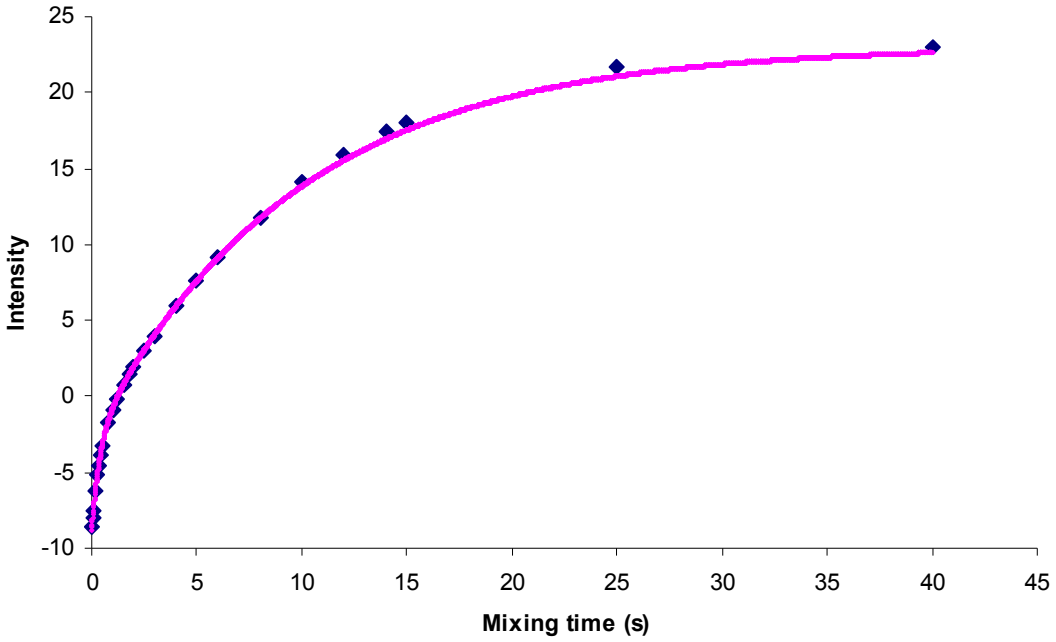

Figure 39. Inversed α-proton (*trans*) for compound **6** at 78°C in D_2O

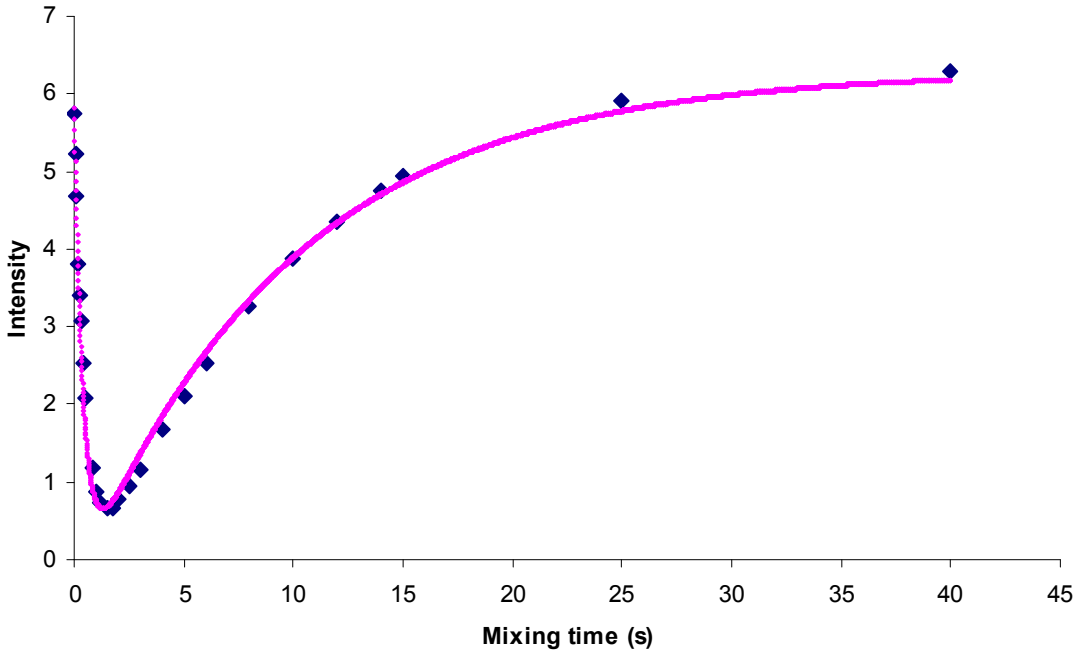

Figure 40. Inversed-recovery α-proton (*cis*) for compound **6** at 78°C in D_2O

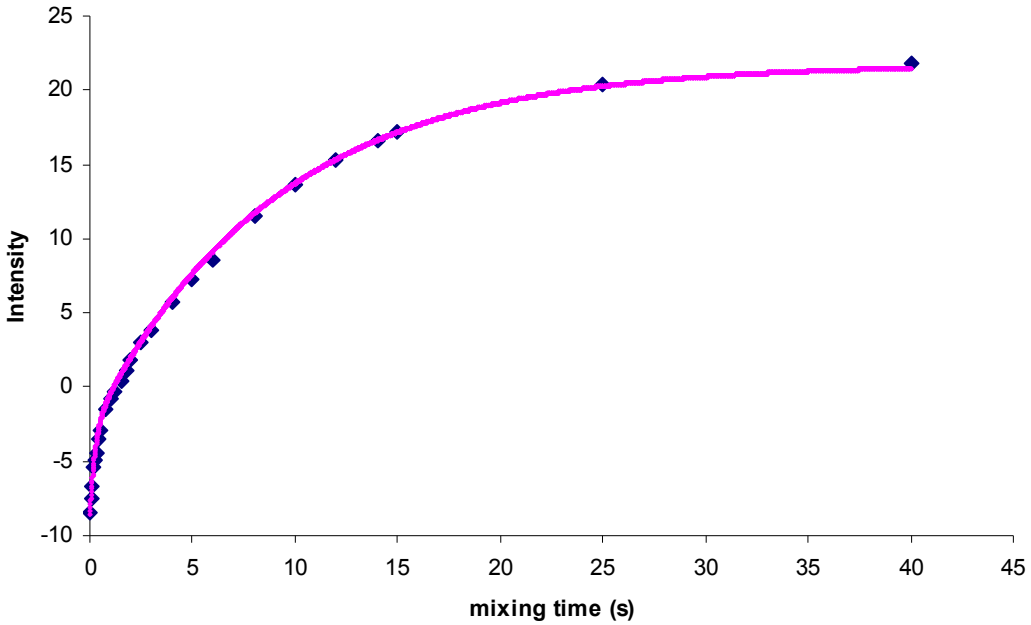

Figure 41. Inversed α-proton (*trans*) for compound **6** at 83°C in D_2O

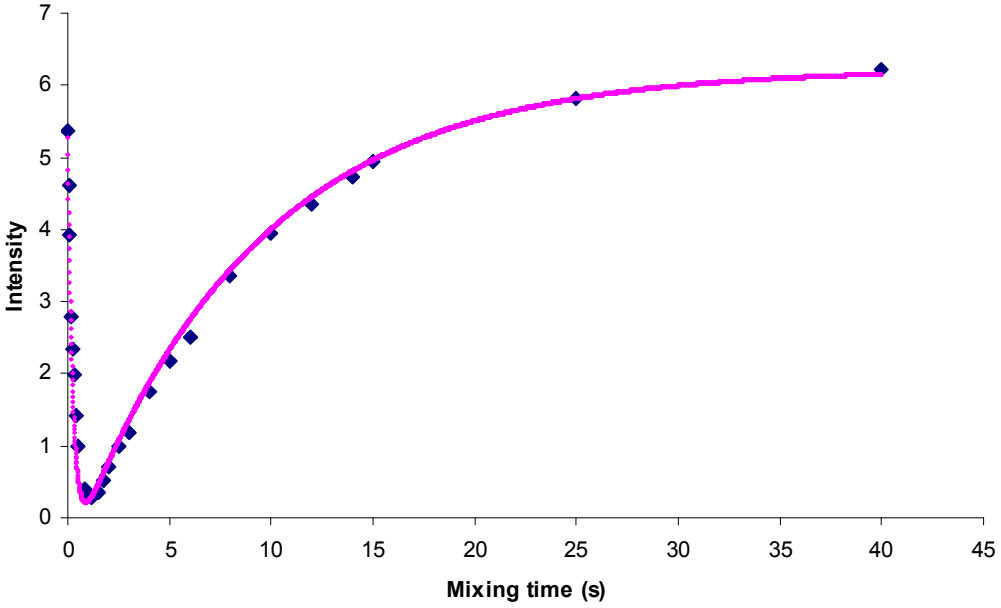

Figure 42. Inversed-recovery α-proton (*cis*) for compound **6** at 83°C in D_2O

Table 1. Data for Inversion-Magnetization Transfer Experiment

Temp. (°C)		93	91	89	86	83	81	78	73	67	62	57	52	46
Temp. (K)		366	364	362	359	356	354	351	346	340	335	330	325	319
3	k_{ct}	0.494	0.400	0.324	0.255	0.182	-	-	-	-	-	-	-	-
	k_{tc}	0.208	0.169	0.135	0.107	0.076	-	-	-	-	-	-	-	-
4	k_{ct}	-	-	-	-	16.186	-	-	-	4.240	2.984	1.592	0.966	0.554
	k_{tc}	-	-	-	-	19.820	-	-	-	5.118	3.125	1.949	1.184	0.679
5	k_{ct}	-	-	4.347	-	2.634	-	1.669	1.053	-	0.363	-	-	-
	k_{tc}	-	-	1.632	-	1.022	-	0.610	0.390	-	0.139	-	-	-
6	k_{ct}	-	-	-	-	2.947	-	1.812	1.111	0.666	0.386	-	-	-
	k_{tc}	-	-	-	-	0.818	-	0.497	0.295	0.177	0.102	-	-	-

Table 2. Equations for *Eyring* plots

Compd	Equation	Slope ± SE	Intercept ± SE
3	*Cis-trans* y = -13.15 x + 29.34	-13.15 ± 0.08	29.33 ± 0.22
	Trans-cis y = -13.30 x + 28.88	-13.30 ± 0.08	28.88 ± 0.22
4	*Cis-trans* y = -9.96 x + 24.86	-9.96 ± 0.06	24.86 ± 0.18
	Trans-cis y = -9.85 x + 24.73	-9.85 ± 0.08	24.73 **±** 0.26
5	*Cis-trans* y = -10.86 x + 25.58	-10.86 ± 0.12	25.58 ± 0.35
	Trans-cis y = -10.83 x + 24.54	-10.83 ± 0.13	24.54 ± 0.38
6	*Cis-trans* y = -11.04 x + 26.18	-11.04 ± 0.04	26.18 ± 0.13
	Trans-cis y = -11.33 x + 25.71	-11.33 ± 0.05	25.71 ± 0.15

$\Delta H^{\neq}$, $\Delta S^{\neq}$, $\Delta G^{\neq}$ were calculated by the following equations:

$\Delta H^{\neq}$ = Slope x R x 1000, $\quad \Delta(\Delta H^{\neq})$ = (ΔSlope) x R (3)

$\Delta S^{\neq}$ = (Intercept – $Ln(k_B/h)$) x R, $\quad \Delta(\Delta S^{\neq})$ = (ΔIntercept) x R (4)

$\Delta G^{\neq} = \Delta H^{\neq} - T\Delta S^{\neq}$ $\quad \Delta(\Delta G^{\neq}) = \Delta(\Delta H^{\neq}) + T\Delta(\Delta S^{\neq})$ (5)

R = 8.3145. $k_B = 1.381 \cdot 10^{-23}$ J·K^{-1}, $h = 6.626 \cdot 10^{-34}$ J·s

Thermodynamics. The equilibrium constants for the interconversion of the *cis* and *trans* isomers of **3-6** were determined by measuring the peak area of the 1H resonance for the two isomers. Peak areas were measured with the program Spinworks 2.5. Experiments were conducted at 298-360 K. Equilibrium constants ($K_{t/c}$ = *trans*/*cis* ratios) were calculated directly from the peak areas.

Table 3. Data for various temperature NMR experiments

Ln$K_{(t/c)}$ values for compounds **3-6** at various temperatures

Temperature (^oC)	93	91	89	86	83	81	78	73	67	62	51	41	30	25
Temperature (K)	366	364	362	359	356	354	351	346	340	335	324	314	303	298
1/T X 10^3	2.732	2.747	2.762	2.786	2.809	2.825	2.849	2.890	2.941	2.985	3.086	3.185	3.300	3.356
3	0.788	-	0.859	-	0.900	-	-	0.952	-	-	1.105	1.211	-	1.335
4	-	-0.136	-	-0.144	-	-0.172	-	-0.203	-	-0.246	-0.236	-0.248	-0.288	-0.294
5	-	-	1.258	-	1.286	-	1.316	1.348	-	1.401	1.442	1.562	-	1.586
6	-	-	-		1.330	-	1.361	1.394	1.428	1.463	1.526	1.581	1.639	1.664

*Ln*K(t/c) values for , Ac-3(*S*)-GlcPro-OMe(**3**),Ac-3(*R*)-GlcPro-OMe(**4**) Ac-3(*S*)-OH-Pro-OMe (**5**) and Ac-Pro-OMe (**6**)

Table 4. *Van't Hoff* plots for $K_{t/c}$

Compd	Equation	Slope ± SE	Intercept ± SE
3	y = 0.838 x - 1.475	0.838 ± 0.033	-1.475 ± 0.010
4	y = -0.247 x + 0.527	-0.247 ± 0.028	0.527 ± 0.085
5	y = 0.546 x – 0.242	0.546 ± 0.014	- 0.242 ± 0.042
6	y = 0.607 x – 0.361	0.607 ± 0.019	-0.361 ± 0.060

ΔH^o, ΔS^o, ΔG^o were calculayed by the following equations:

ΔH^o = slope x R x 1000, $\Delta(\Delta H^o) = \Delta$slope x R (6)

ΔS^o = intercept x R, $\Delta(\Delta S^o) = \Delta$intercept x R (7)

$\Delta G^o = \Delta H^o - T\Delta S^o$ $\Delta(\Delta G^o) = \Delta(\Delta H^o) + T\Delta(\Delta S^o)$ (8)

R = 8.3145.

FT-IR spectroscopy. Samples of **3-6** were prepared at concentration of 0.10 M in D_2O. Spectra were recorded on a FTIR spectrometer. Experiments were performed at 25 ^oC using CaF_2 in a Spectra Tech circle cell. The frequency of amide I vibrational modes was determined to within 2 cm^{-1}.

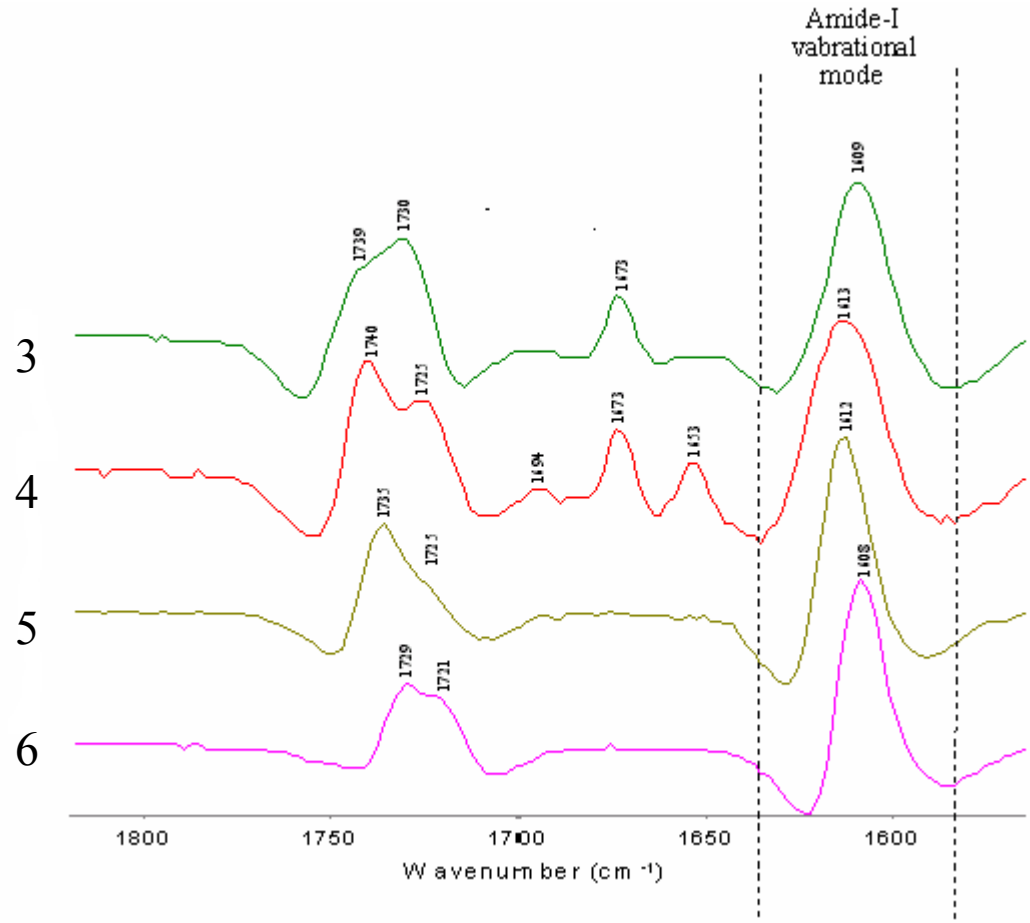

Figure 43. FT-IR spectra of amide-I (C=O) vibrational mode for compounds **3-6**.

Temperature coefficient (Δδ/ΔT) experiment: 1 D ^{1}H-NMR spectroscopy of 17mM solutions of **3** and **4** in 100.0% Me_2SO-d_6 were recorded on 500MHz NMR spectrometer at 20 ^oC, and from 20 to 45 ^oC with increments of 5 ^oC, using routine techniques. Chemical shift (δ) are expressed in ppm and calibrated with respect to the residual DMSO signal (^{1}H: 2.49 ppm).

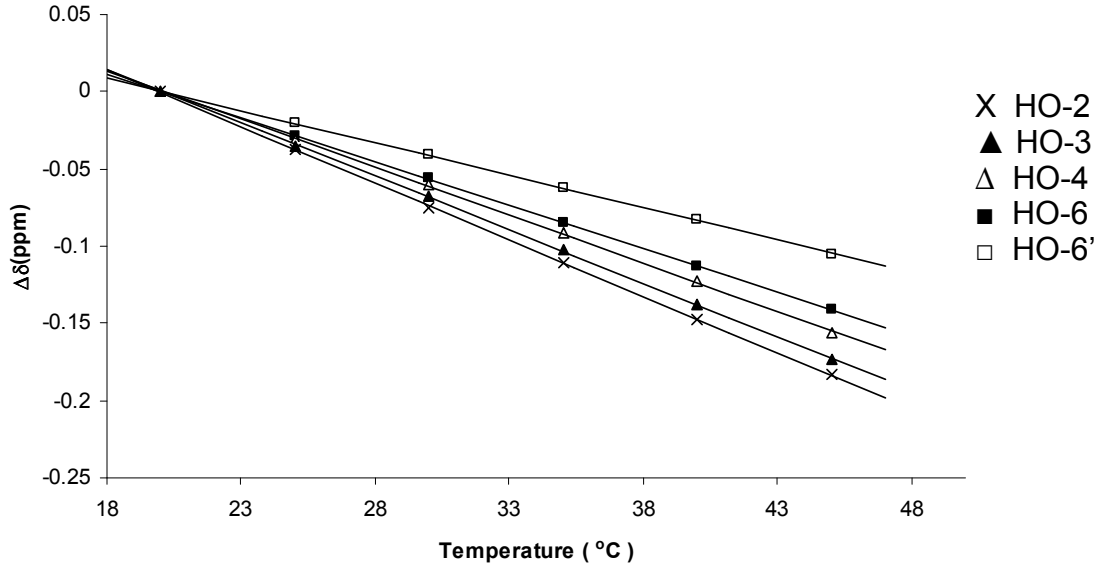

Figure 44. Temperature dependence of hydroxyl proton resonances of the *cis* isomer of Ac-3'(*R*)-GlcPro-OMe (**3**) in DMSO-d_6.

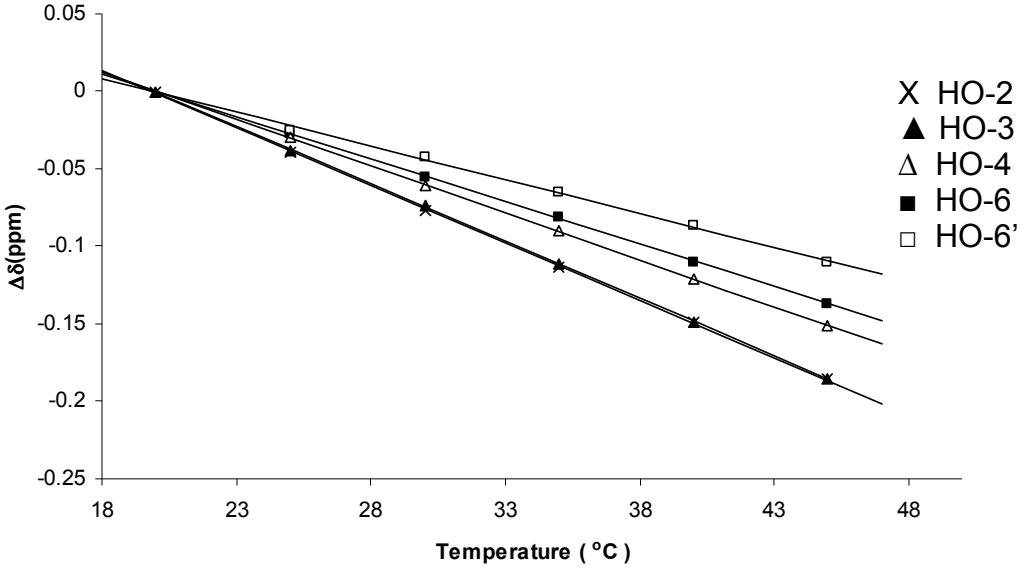

Figure 45. Temperature dependence of hydroxyl proton resonances of the *trans* isomer of Ac-3'(*R*)-GlcPro-OMe (**3**) in DMSO-d_6.

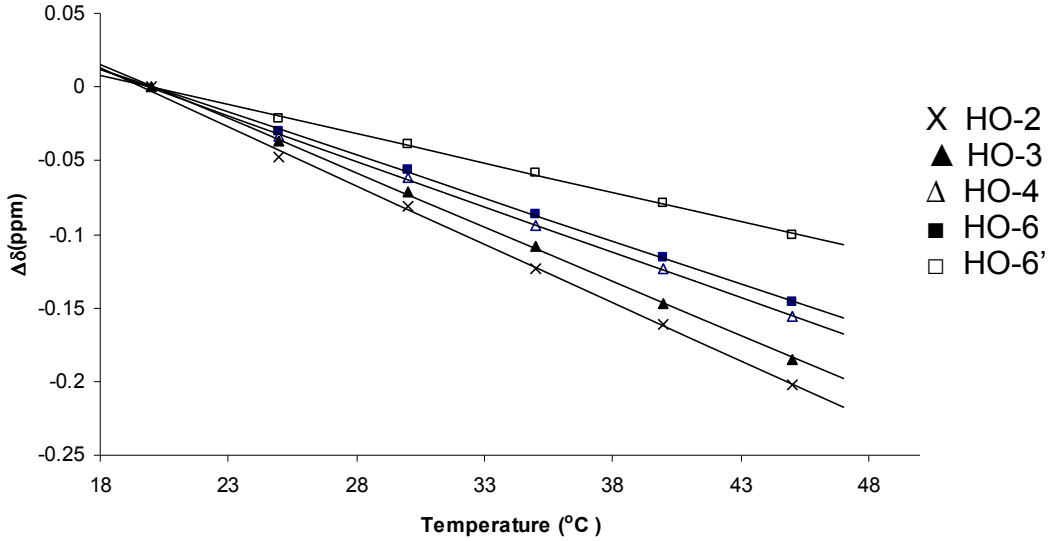

Figure 46 Temperature dependence of hydroxyl proton resonances of the *cis* isomer of Ac-3'(*R*)-GlcPro-OMe (**4**) in DMSO-d_6.

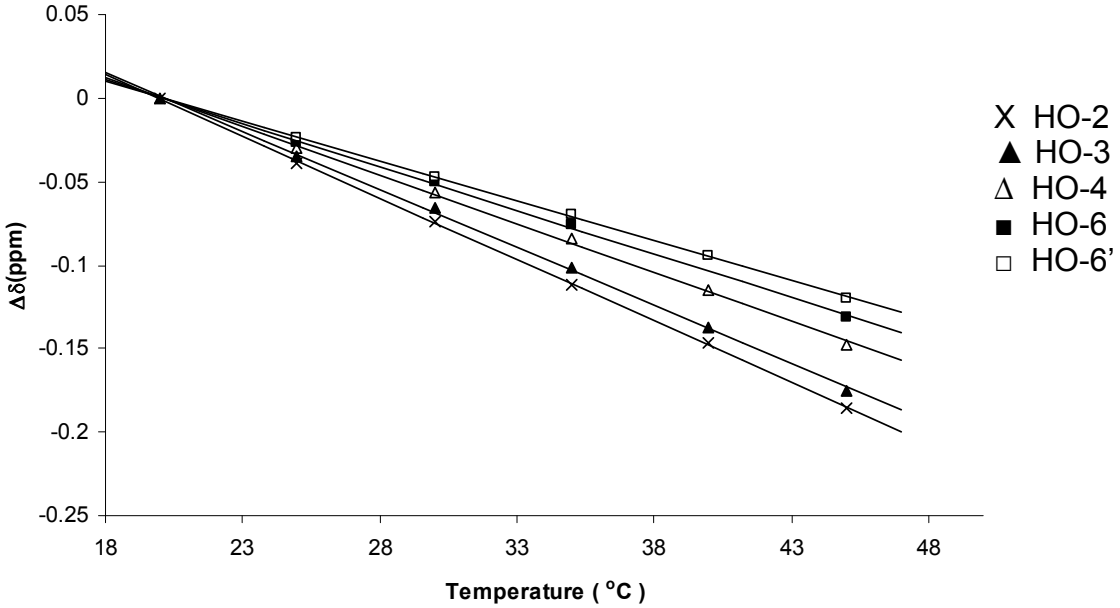

Figure 47. Temperature dependence of hydroxyl proton resonances of the *trans* isomer of Ac-3'(*R*)-GlcPro-OMe (**4**) in DMSO-d_6.

Computational Methods

A computational approach was used for detailed structural assignments and determination of the conformational distributions of compounds **3** and **4** in water. Due to the complexity of the potential energy surface of these compounds, a systematic conformational search routine was employed. First, the MMFF94 force field implemented in the SPARTAN '02 program was used to generate an initial set of trial structures or conformers. Specifically, a Monte-Carlo or random conformational search was performed starting from an initial energy minimized guess structure drawn in SPARTAN. Although Monte-Carlo was designed to fairly sample all regions of the conformational space, one cannot guarantee that all lowest energy conformers are located. As a result of this limitation in the random sampling technique, some very important conformers might be missed during the search. To avoid this inherent problem, we adopted a strategy of searching the conformational space by re-starting the search with different initial conformations and checking for the completeness of the analysis. Once a redundant outcome was observed, we assumed that the conformational space was fully covered and the conformations were gathered. This 'build and search' approach identified a set of 2700 structures for each compound (**3** and **4**). However, when these structures were superimposed, a set of 443 unique conformers for compound **3** and 457 for compound **4** were isolated.

Once the unique local minima were identified using MMFF94, the remaining conformers were used as guess structures (input structures) for gas phase B3LYP/6-31+G(d, p) optimizations as implemented in the GAUSSIAN 03 program package[1]. Full B3LYP/6-31+G(d, p) optimizations lead to 443 and 453 unique conformers for compounds **3** and **4**, respectively. All B3LYP structures were real local minima as characterized by the absence of imaginary frequencies.

Subsequently, solvent effects were taken into account through re-optimization of the gas-phase B3LYP/6-31+G(d, p) minima in water at the same level of theory using Tomasi's Polarized Continuum Model (PCM). This led to only 355 and 258 real local minima for compounds **3** and **4**, respectively.

The remaining structures either had large imaginary frequencies, which were very difficult to avoid, or the structures were difficult to converge. When the SCF convergence behavior for structures with convergence problems was checked by analyzing the energy change for each iterative step, it was found that there is no dramatic change in their energy from one step to the next. Moreover, these structures are at a higher energy level compared to the collected conformers, which suggests that they are relatively unimportant for our total analysis. Thus, such structures were discarded after repeated attempts to reach convergence had failed.

Using the B3LYP optimized geometries in water, the total free energies of each conformer were calculated. The total free energies were subsequently used to determine the *cis*/*trans* ratio of the local minima according to a Boltzmann distribution (Boltzmann statistics) calculated at 25 ºC. In Tables 5 and 6, we report data for the most stable conformers **3** and **4**. Only those conformers have been listed in the tables that have a statistical weight of at least 0.5%, according to the Boltzmann distribution. For each conformer, we provide the total energy, statistical weight, as well as various torsion angles (key geometry parameters.) The calculated dipole moment has been included for future reference since it has a strong influence on the free energy of solvation.

TABLE 5: Backbone Torsion Angles, Endocyclic Torsion Angles, and Conformational Distribution of Cis-Trans Isomers of Compound 3, which are optimized at the B3LYP/6-31+G(d) Level of Theory in the Water.

Conformers	B3LYP/6-31+G(d)		Dipole moment [b]	Backbone Torsion Angles and Endocyclic Torsion Angles [a]								
	H_2O (a.u.) Total Free Energy	Conformer Distribution	In H_2O	ω'	ϕ	ψ	ω	χ^1	χ^2	χ^3	χ^4	χ^0
Conformer1	-1279.15805900	4.70017076	5.1329	175.253	-64.198	153.736	177.502	28.915	-34.773	26.879	-8.378	-13.164
Conformer2	-1279.15797400	4.29548658	5.6868	174.849	-63.973	153.458	177.498	29.437	-34.414	25.781	-6.852	-14.482
Conformer3	-1279.15786500	3.82710817	7.6872	175.55	-61.41	-28.681	-179.498	27.616	-33.469	26.027	-8.356	-12.356
Conformer4	-1279.15761700	2.94297812	8.8327	175.706	-61.659	-28.731	-179.405	28.154	-34.144	26.603	-8.633	-12.497
Conformer5	-1279.15749700	2.59170305	9.6162	175.751	-61.884	-28.605	-179.79	28.405	-34.608	27.1	-8.983	-12.439
Conformer6	-1279.15748700	2.56439600	5.7266	175.486	-61.371	-28.421	-178.709	27.881	-33.682	26.107	-8.272	-12.569
Conformer7	-1279.15748500	2.55896921	6.6757	174.313	-64.422	153.418	177.149	30.688	-34.505	24.71	-4.861	-16.547
Conformer8	-1279.15744600	2.45541259	6.9431	174.809	-63.748	153.48	177.554	29.199	-34.614	26.354	-7.622	-13.835
Conformer9	-1279.15733500	2.18304566	7.5057	176.059	-61.619	-29.02	-179.011	27.947	-34.48	27.349	-9.547	-11.775
Conformer10	-1279.15718900	1.87025420	12.0112	177.627	-67.256	154.625	176.597	27.487	-33.487	26.314	-8.613	-12.088
Conformer11	-1279.15718800	1.86827423	10.7905	-10.903	-63.708	154.37	177.909	31.884	-34.728	23.936	-3.193	-18.36
Conformer12	-1279.15716100	1.81560020	7.8150	174.055	-64.29	153.729	177.029	30.79	-34.36	24.383	-4.444	-16.879
Conformer13	-1279.15711000	1.72012283	7.2059	175.399	-61.183	-29.02	-179.311	28.093	-33.767	26.084	-8.126	-12.779
Conformer14	-1279.15705000	1.61420453	7.5512	-10.713	-64.058	153.755	177.811	31.792	-34.917	24.354	-3.726	-17.943
Conformer15	-1279.15704400	1.60397824	7.5835	-10.972	-63.957	154.078	177.621	31.89	-35.01	24.411	-3.721	-18.01
Conformer16	-1279.15700800	1.54396672	11.3666	177.548	-66.781	154.711	177.005	27.948	-33.772	26.306	-8.315	-12.573
Conformer17	-1279.15696000	1.46742941	8.3907	-10.68	-62.642	-27.379	-177.946	30.963	-34.117	23.815	-3.727	-17.428
Conformer18	-1279.15685100	1.30742140	5.3364	-10.749	-63.601	153.891	177.725	31.447	-34.857	24.607	-4.229	-17.401
Conformer19	-1279.15682900	1.27730691	7.4783	175.365	-61.205	-29.374	-178.796	28.155	-33.865	26.186	-8.187	-12.779
Conformer20	-1279.15674100	1.16362742	8.7979	175.163	-61.389	-28.169	-179.668	28.332	-34.102	26.377	-8.261	-12.856
Conformer21	-1279.15672900	1.14893052	6.7307	-9.63	-62.972	-27.043	-177.84	30.548	-34.302	24.547	-4.794	-16.464
Conformer22	-1279.15669700	1.11063994	10.8316	-1.733	-70.669	153.388	177.641	33.395	-35.71	23.807	-2.004	-20.045
Conformer23	-1279.15669000	1.10243549	9.4318	178.559	-64.409	-27.738	-179.68	26.06	-33.108	27.07	-10.435	-9.993
Conformer24	-1279.15668300	1.09429164	3.8631	-9.77	-62.77	-27.496	-177.25	30.428	-34.185	24.488	-4.807	-16.378
Conformer25	-1279.15666800	1.07704254	10.8443	-1.876	-71.231	153.371	177.594	33.611	-35.857	23.82	-1.878	-20.26

Conformer26	-1279.15665800	1.06569446	5.4082	-9.889	-62.33	-27.827	-177.096	30.101	-33.876	24.28	-4.792	-16.197
Conformer27	-1279.15664700	1.05334962	10.8863	170.248	-56.04	-29.592	-178.56	26.461	-35.759	30.851	-14.224	-7.808
Conformer28	-1279.15663300	1.03784461	8.3676	169.778	-59.198	153.487	176.826	28.366	-36.2	29.719	-11.737	-10.635
Conformer29	-1279.15661600	1.01932360	4.5373	175.556	-60.875	-29.808	-178.657	27.684	-33.658	26.29	-8.615	-12.196
Conformer30	-1279.15660500	1.00751591	10.1026	177.233	-66.961	154.345	176.976	27.794	-33.45	25.946	-8.031	-12.662
Conformer31	-1279.15658100	0.98222629	5.4440	174.626	-64.115	151.95	175.367	30.419	-34.763	25.404	-5.81	-15.773
Conformer32	-1279.15656400	0.96469783	14.3113	-3.291	-70.535	153.12	177.54	33.483	-34.36	21.596	0.389	-21.651
Conformer33	-1279.15655600	0.95655772	10.1262	169.712	-55.97	-29.472	-178.615	26.193	-34.771	29.505	-12.975	-8.458
Conformer34	-1279.15654500	0.94547711	8.5896	165.447	-53.435	-29.854	-178.172	25.884	-34.453	29.298	-12.975	-8.285
Conformer35	-1279.15654300	0.94347629	10.1153	175.362	-61.039	-28.822	-178.998	27.718	-33.497	26	-8.297	-12.419
Conformer36	-1279.15649400	0.89575709	9.3623	166.129	-53.334	-30.287	-178.387	25.099	-34.786	30.63	-14.909	-6.521
Conformer37	-1279.15644400	0.84955111	10.4472	178.633	-63.984	-28.88	-178.987	25.955	-33.168	27.273	-10.711	-9.749
Conformer38	-1279.15643900	0.84506368	8.4195	-9.329	-62.914	-27.107	-178.164	30.355	-34.682	25.333	-5.75	-15.738
Conformer39	-1279.15642200	0.82998297	9.1869	164.495	-56.344	152.993	176.97	28.09	-36.156	29.88	-12.072	-10.264
Conformer40	-1279.15642100	0.82910430	10.1977	171.153	-56.406	-29.716	-177.731	25.545	-35.246	30.974	-14.96	-6.759
Conformer41	-1279.15638400	0.79723914	9.6697	165.788	-53.402	-30.686	-177.616	25.705	-34.994	30.4	-14.258	-7.327
Conformer42	-1279.15636600	0.78218295	9.7219	175.849	-61.72	-28.977	-179.497	28.244	-34.288	26.771	-8.747	-12.481
Conformer43	-1279.15636400	0.78052769	8.4203	-9.462	-62.976	-27.188	-177.981	30.484	-34.706	25.239	-5.549	-15.954
Conformer44	-1279.15632300	0.74735630	9.7530	165.884	-53.481	-30.46	-177.374	25.903	-35.11	30.379	-14.095	-7.55
Conformer45	-1279.15628600	0.71863299	11.2931	170.369	-56.445	-29.143	-178.101	25.724	-34.231	29.135	-12.9	-8.21
Conformer46	-1279.15628300	0.71635303	13.8887	-3.24	-70.809	153.498	177.347	33.778	-34.389	21.342	0.857	-22.13
Conformer47	-1279.15627900	0.71332434	7.9777	171.237	-56.629	-29.889	-177.841	25.746	-35.368	30.976	-14.84	-6.959
Conformer48	-1279.15625400	0.69468300	13.8661	-3.404	-71.046	153.163	177.505	33.693	-34.427	21.477	0.671	-21.966
Conformer49	-1279.15624900	0.69101360	7.1810	-11.075	-63.19	-28.213	-177.649	31.159	-33.869	23.237	-2.969	-18.044
Conformer50	-1279.15624600	0.68882127	9.3977	163.635	-56.031	153.751	176.631	28.087	-35.191	28.346	-10.447	-11.319
Conformer51	-1279.15621300	0.66515990	4.8429	-9.645	-62.458	-27.128	-177.416	30.071	-33.976	24.521	-5.094	-15.955
Conformer52	-1279.15621000	0.66304959	8.3825	176.054	-61.66	-28.593	-179.731	27.959	-34.37	27.172	-9.35	-11.914
Conformer53	-1279.15619500	0.65259808	11.2403	-3.017	-71.674	153.034	177.422	34.082	-34.889	21.823	0.551	-22.121
Conformer54	-1279.15617400	0.63824214	6.6183	165.996	-53.495	-30.433	-177.748	25.711	-35.112	30.56	-14.43	-7.214
Conformer55	-1279.15069300	0.63756646	2.8566	176.006	-41.743	132.539	178.252	-5.605	-14.717	29.215	-34.55	-25.528
Conformer56	-1279.15614100	0.61631819	7.9141	178.168	-63.316	-28.592	-178.828	25.386	-32.416	26.629	-10.42	-9.571
Conformer57	-1279.15614000	0.61566571	8.3052	-11.703	-64.354	153.877	177.66	32.655	-34.571	22.943	-1.625	-19.854
Conformer58	-1279.15610900	0.59577806	9.0827	165.159	-53.272	-30.275	-177.498	25.87	-34.411	29.246	-12.924	-8.307

Conformer59	-1279.15607500	0.57470371	10.3456	165.331	-53.511	-29.889	-177.981	25.949	-34.447	29.227	-12.867	-8.384
Conformer60	-1279.15606900	0.57106285	7.5206	-10.037	-62.966	-27.543	-177.851	30.931	-34.588	24.616	-4.611	-16.84
Conformer61	-1279.15605800	0.56444775	11.9053	165.703	-53.206	-29.521	-177.935	25.342	-34.881	30.585	-14.715	-6.792
Conformer62	-1279.15604300	0.55555047	11.3924	165.649	-53.595	-29.54	-178.976	25.893	-35.017	30.236	-13.973	-7.642
Conformer63	-1279.15599500	0.52801080	8.9909	170.236	-56.546	-29.551	-177.579	25.492	-34.176	29.308	-13.26	-7.839
Conformer64	-1279.15598100	0.52023862	6.9900	-1.77	-70.445	-28.226	-177.256	32.8	-35.235	23.58	-2.187	-19.525
Others*		< 0.5										

Total Population Distribution

	Calc.(%)	Exp. (%)
Total Cis Isomers	**29.15**	**23**
Total Trans Isomers	**70.85**	**77**

[a] angles are in degrees, [b] units in Debye (D). The relative electronic energies and the relative free energies are in Hartrees. The population distributions were calculated using the Boltzmann statistical weights at 25 °C, including all conformers. In the property table, only those conformers are included that contribute 0.5% or more.

TABLE 6: Backbone Torsion Angles, Endocyclic Torsion Angles, and Conformational Distribution of Cis-Trans Isomers of Compound 4, which is Optimized at the B3LYP/6-31+G(d) Level of Theory in the Water

Conformers	B3LYP/6-31+G(d)		Dipole moment [b]	Backbone Torsion Angles and Endocyclic Torsion Angles [a]								
	H2O (a.u.) Total Free Energy	Conformer Distribution	In H2O	ω'	ϕ	ψ	ω	χ^1	χ^2	χ^3	χ^4	χ^0
Conformer1	-1279.15838500	4.15042264	10.9153	4.031	-81.347	154.516	176.927	32.683	-37.378	27.191	-6.035	-16.964
Conformer2	-1279.15837300	4.09800180	11.0304	4.297	-80.845	154.838	177.406	32.539	-37.457	27.452	-6.399	-16.641
Conformer3	-1279.15835700	4.02913580	4.9618	-170.077	-85.486	154.199	177.889	32.851	-33.196	20.473	1.061	-21.596
Conformer4	-1279.15822100	3.48858953	10.13710	3.902	-82.254	154.02	177.165	32.835	-37.137	26.661	-5.391	-17.464
Conformer5	-1279.15808700	3.02696829	6.5048	-172.554	-82.246	154.897	178.008	59.846	-30.292	18.116	2.039	-20.834
Conformer6	-1279.15801200	2.79580419	10.9310	3.878	-79.31	154.78	177.459	31.566	-36.457	26.859	-6.415	-16.019
Conformer7	-1279.15800500	2.77515118	10.9293	3.926	-78.782	153.309	177.545	31.75	-36.739	27.139	-6.59	-16.015
Conformer8	-1279.15796200	2.65158775	12.5069	4.344	-81.073	154.429	176.76	32.373	-37.373	27.468	-6.529	-16.447
Conformer9	-1279.15795800	2.64037702	6.5169	-172.448	-82.232	154.292	179.353	30.499	-30.342	18.261	1.836	-20.648
Conformer10	-1279.15791500	2.52281441	7.8114	-172.917	-81.541	154.684	178.19	30.176	-29.97	18.004	1.879	-20.468
Conformer11	-1279.15781500	2.26925765	5.1614	-170.53	-86.917	153.504	177.346	33.723	-33.628	20.387	1.719	-22.572
Conformer12	-1279.15772300	2.05855481	13.7801	4.2	-79.496	154.916	176.881	31.871	-37.151	27.642	-7.035	-15.814
Conformer13	-1279.15770400	2.01753998	8.3455	3.512	-81.193	-28.105	-177.812	32.361	-36.72	26.421	-5.464	-17.112

Conformer14	-1279.15767700	1.96065755	5.1522	-170.208	-86.394	153.91	177.6	33.493	-33.659	20.655	1.279	-22.147
Conformer15	-1279.15756000	1.73212807	9.7505	12.897	-91.14	154.666	177.338	32.641	-33.236	20.844	0.606	-21.173
Conformer16	-1279.15752900	1.67617568	9.7577	12.757	-90.437	154.79	177.186	32.551	-33.191	20.854	0.538	-21.074
Conformer17	-1279.15742100	1.49498874	7.5951	4.217	-79.003	-27.526	-177.594	31.29	-36.44	27.064	-6.843	-15.553
Conformer18	-1279.15738000	1.43145372	8.4981	4.245	-80.608	-28.347	-177.15	31.629	-36.286	26.438	-5.955	-16.341
Conformer19	-1279.15737900	1.42993829	8.7994	4.529	-82.05	152.858	175.989	32.954	-37.887	27.75	-6.464	-16.866
Conformer20	-1279.15736500	1.40889000	7.2791	-170.052	-84.046	-27.779	-179.098	32.501	-32.811	20.21	1.031	-21.333
Conformer21	-1279.15734600	1.38081915	8.5042	3.915	-80.778	-28.379	-177.398	31.934	-36.576	26.596	-5.929	-16.544
Conformer22	-1279.15732300	1.34758590	5.9159	4.935	-78.149	-27.92	-177.228	31.189	-37.028	28.108	-8.014	-14.737
Conformer23	-1279.15721800	1.20574339	6.8370	12.555	-90.425	154.631	177.253	32.497	-32.985	20.554	0.81	-21.207
Conformer24	-1279.15721400	1.20064559	7.6057	4.62	-80.305	-28.143	-177.458	32.019	-37.135	27.458	-6.787	-16.038
Conformer25	-1279.15720500	1.18925420	5.9903	3.744	-80.935	-28.491	-177.344	32.074	-36.59	26.508	-5.756	-16.736
Conformer26	-1279.15714100	1.18925420	9.3605	4.276	-77.968	-27.479	-177.297	31.037	-36.672	27.67	-7.642	-14.882
Conformer27	-1279.15713400	1.10309683	8.0443	12.314	-90.783	153.222	177.425	33.237	-34.026	21.54	0.256	-21.331
Conformer28	-1279.15712300	1.09031872	6.3277	-171.984	-81.833	154.82	178.388	30.76	-31.456	19.83	0.343	-19.863
Conformer29	-1279.15711100	1.07654773	7.4730	-170.08	-83.735	-28.796	-178.569	32.442	-33.185	20.865	0.318	-20.84
Conformer30	-1279.15708100	1.04287641	11.0267	12.45	-90.565	154.9	177.356	32.588	-33.336	21.051	0.357	-20.977
Conformer31	-1279.15706700	1.02752556	5.6968	-171.645	-79.531	-26.81	-179.607	30.626	-31.461	19.901	0.15	-19.636
Conformer32	-1279.15701000	0.96732360	9.6433	-170.626	-84.75	154.602	177.906	32.227	-32.33	19.761	1.395	-21.428
Conformer33	-1279.15700700	0.96425464	9.6433	4.865	-79.122	-28.789	-176.825	31.377	-36.812	27.568	-7.32	-15.299
Conformer34	-1279.15695900	0.91645474	9.2865	-169.534	-84.422	-27.317	-179.049	32.379	-33.319	21.169	-0.052	-20.571
Conformer35	-1279.15695800	0.91548452	6.7779	-171.356	-82.268	153.853	179.034	31.428	-32.728	21.177	-0.623	-19.657
Conformer36	-1279.15689600	0.85729458	8.6034	-170.132	-85.569	153.411	-179.818	32.805	-33.005	20.231	1.281	-21.716
Conformer37	-1279.15688700	0.84916081	12.0283	3.931	-82.023	153.88	177.72	33.075	-37.619	27.186	-5.76	-17.401
Conformer38	-1279.15686200	0.82696965	5.6947	-171.096	-82.727	154.418	177.761	31.508	-33.04	21.605	-1.014	-19.463
Conformer39	-1279.15684500	0.81221184	9.3748	11.487	-91.737	154.783	177.15	32.743	-32.909	20.221	1.309	-21.674
Conformer40	-1279.15679100	0.76705854	7.3595	-170.138	-85.506	154.067	178.014	33.061	-33.416	20.64	1.023	-21.699
Conformer41	-1279.15678100	0.75897656	5.8700	-171.742	-82.677	154.286	177.643	31.176	-31.666	19.763	0.694	-20.348
Conformer42	-1279.15670000	0.69657383	7.6156	-169.538	-83.9	-28.409	-178.713	32.12	-33.097	21.07	-0.119	-20.361
Conformer43	-1279.15668100	0.69657383	8.3135	-171.35	-80.052	-26.936	-179.325	30.15	-31.243	20.044	-0.33	-19.024
Conformer44	-1279.15667000	0.67478699	9.6358	4.091	-81.838	154.139	177.361	32.967	-37.581	27.244	-5.904	-17.226
Conformer45	-1279.15666100	0.66838481	12.3637	11.538	-90.866	155.267	177.139	32.629	-32.982	20.448	0.998	-21.406
Conformer46	-1279.15659900	0.62590100	9.0037	-169.576	-83.957	-27.802	-179.535	32.477	-33.131	20.735	0.47	-20.97

Conformer47	-1279.15655300	0.59613546	13.8152	3.956	-81.412	153.965	177.561	32.564	-37.37	27.294	-6.205	-16.792
Conformer48	-1279.15653600	0.58549704	12.9746	3.907	-82.207	154.239	177.143	32.742	-37.114	26.736	-5.529	-17.326
Conformer49	-1279.15653200	0.58302160	10.3246	-171.452	-84.225	154.551	178.295	31.992	-32.045	19.589	1.414	-21.303
Conformer50	-1279.15650500	0.56658391	9.3459	-170.544	-84.891	154.554	177.422	32.29	-32.307	19.654	1.548	-21.559
Conformer51	-1279.15649400	0.56002069	10.4355	3.759	-82.204	-27.891	-178.006	32.7	-36.942	26.448	-5.26	-17.46
Conformer52	-1279.15645600	0.53792720	12.3176	11.31	-91.845	154.642	176.438	32.758	-32.898	20.179	1.352	-21.704
Conformer53	-1279.15645200	0.53565288	10.2786	-171.622	-83.652	154.359	178.253	31.855	-31.854	19.37	1.568	-21.317
Conformer54	-1279.15643200	0.52442471	5.4632	12.852	-89.47	-28.305	-178.455	32.443	-33.58	21.54	-0.319	-20.44
Conformer55	-1279.15641700	0.51615831	15.1406	4.236	-81.741	153.895	177.438	32.835	-37.567	27.355	-6.103	-17.018
Others*		< 0.5										

Total Population Distribution

	H_2O (%)	**Exp. H_20 (%)**
Total *Cis* Isomers	57.75	53
Total *Trans* Isomers	42.25	47

[a] angles are in degrees, [b] units in Debye (D). The relative electronic energies and the relative free energies are in Hartrees. The population distributions were calculated using the Boltzmann statistical weights at 25 ^{o}C, including all conformers. In the property table, only those conformers are included that contribute 0.5% or more.

Hydrogen Bonds: The most stable conformers were studied for internal hydrogen bonding. For the hydrogen bonding characterization, we used a ≤ 2.5Å bond length cutoff to ensure that only strong hydrogen bonds were selected.[2] We increased the bond distance cutoff from ≤ 2.1Å to ≤ 2.5Å to check the sensitivity of the cutoff. However, the results found from both cutoffs remains the same. Based on this criterion we found two types of hydrogen bonds in those conformers of compounds **3** and **4** that contribute to a population distribution greater > 0.5% (Table 1-2). For compound **3**, the first major hydrogen bond exists between OH-6′ and OH-6 (6′-OH-------OH-6). The average hydrogen bond distance is ≈ 1.9Å. This hydrogen bond was found in prolyl amide *trans* conformers **10, 16, 23, 30, 37** and **56** (Table 5). The second type of hydrogen bond in compound **3**, exists between OH-6′ and *N*-terminal carbonyl (6′-OH-------O=C-N) and is found in the *cis* conformers only. Conformers **22, 25, 32, 46, 48, 53**, and **64** possess this hydrogen bond (Table 5). The bond distance of this hydrogen bond is ≈ 1.8Å. In addition, a third type of hydrogen bond is found between OH-2 and the *C*-terminal carbonyl (2-OH---O=C′-C^{α}) with a bond distance of 1.9Å. This hydrogen bond was found in only one out of 43 *trans* conformers.

For Compound **4**, the first major hydrogen bonding exists between 6′-OH and the *N*-terminal carbonyl (6′-OH---O=C′-N) and the bond distance is ≈ 1.8 Å. These conformers with this kind of hydrogen bond are conformers **1, 2, 4, 6, 7, 8, 12, 13, 17, 18, 19, 21, 22, 25, 33, 37, 44, 47, 48, 51,** and **55** (Table 6). All these above-mentioned twenty-one conformers favor a *cis* prolyl amide structure. The second hydrogen bond exists between 6′-OH and the *C*-terminal carbonyl (C^{δ}-CH_2-OH---O=C′- C^{α}) and is found in both *cis* and *trans* conformations. The conformers with this kind of hydrogen bond that favor the *cis* prolyl amide structure are conformers **15, 16, 23, 30, 39,** and **52** and the conformers that favor the *trans* structure are also conformers **3, 5, 10, 32, 36, 40, 49, 50,** and **53** (Table 6). The bond distance of this hydrogen bonding is ≈ 1.9 Å.

Figure **48** shows the most stable *cis*/*trans* prolyl amide conformer for compound **3** while the most stable *cis*/*trans* prolyl amide conformer for compound **4** is shown in Figure **49**.

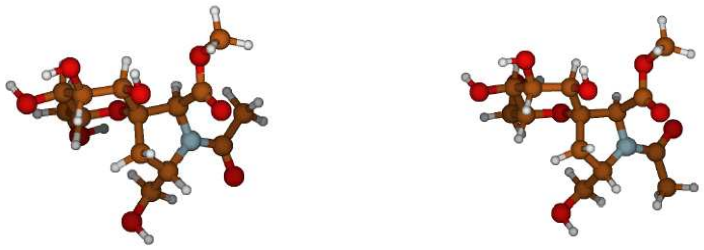

Figure 48. The most stable conformers of compound **3**: the most stable *cis* conformer is shown on the left while the most stable *trans* conformer is shown on the right. In these two conformers no intramolecular hydrogen bond was identified

Figure 49. The most stable conformers of compound **4**: the most stable *cis* conformer is shown on the left while the most stable *trans* conformer is on the right. The intramolecular hydrogen bonds between 6′-OH ···· O=C-N (*cis* isomer) and 6′-OH ···· O=C-C^{α} are indicated.

References

(1) Frisch, M. J.; Trucks, G. W.; Schlegel, H. B.; Scuseria, G. E.; Robb, M. A.; Cheeseman, J. R.; Montgomery, J. A.; Vreven, T.; Kudin, K. N.; Burant, J. C.; Millam, J. M.; Iyengar, S. S.; Tomasi, J.; Barone, V.; Mennucci, B.; Cossi, M.; Scalmani, G.; Rega, N.; Petersson, G. A.; Nakatsuji, H.; Hada, M.; Ehara, M.; Toyota, K.; Fukuda, R.; Hasegawa, J.; Ishida, M.; Nakajima, T.; Honda, Y.; Kitao, O.; Nakai, H.; Klene, M.; Li, X.; Knox, J. E.; Hratchian, H. P.; Cross, J. B.; Bakken, V.; Adamo, C.; Jaramillo, J.; Gomperts, R.; Stratmann, R. E.; Yazyev, O.; Austin, A. J.; Cammi, R.; Pomelli, C.; Ochterski, J. W.; Ayala, P. Y.; Morokuma, K.; Voth, G. A.; Salvador, P.; Dannenberg, J. J.; Zakrzewski, V. G.; Dapprich, S.; Daniels, A. D.; Strain, M. C.; Farkas, O.; Malick, D. K.; Rabuck, A. D.; Raghavachari, K.; Foresman, J. B.; Ortiz, J. V.; Cui, Q.; Baboul, A. G.; Clifford, S.; Cioslowski, J.;

Stefanov, B. B.; Liu, G.; Liashenko, A.; Piskorz, P.; Komaromi, I.; Martin, R. L.; Fox, D. J.; Keith, T.; Al-Laham, M. A.; Peng, C. Y.; Nanayakkara, A.; Challacombe, M.; Gill, P. M. W.; Johnson, B.; Chen, W.; Wong, M. W.; Gonzalez, C.; Pople, J. A. Gaussian 03, revision D.02; Gaussian, Inc.: Wallingford CT, 2004.

(2) Morozov, A.; Kortemme, T.; Tsemekhman, K.; Baker, D. *Proc. Natl. Acad. Sci. U S A* **2004**. *101*, 6946.